

SPECIAL ISSUE ARTICLE

New digital braincase endocasts of two species of *Desmotosuchus* and neurocranial diversity within Aetosauria (Archosauria: Pseudosuchia)

M. Belén von Baczko^{1,2}  | Julia. B. Desojo^{2,3}  | David J. Gower⁴ |
 Ryan Ridgely⁵ | Paula Bona^{2,3}  | Lawrence M. Witmer⁵ 

¹Sección Paleontología de Vertebrados, Museo Argentino de Ciencias Naturales “Bernardino Rivadavia”, Ciudad Autónoma de Buenos Aires, Argentina

²Consejo Nacional de Investigaciones Científicas y Técnicas (CONICET), Ciudad Autónoma de Buenos Aires, Argentina

³División Paleontología Vertebrados, Facultad de Ciencias Naturales y Museo, Universidad Nacional de La Plata, La Plata, Argentina

⁴Department of Life Sciences, The Natural History Museum, London, UK

⁵Department of Biomedical Sciences, Ohio Center for Ecology and Evolutionary Biology, Heritage College of Osteopathic Medicine, Ohio University, Athens, Ohio, USA

Correspondence

M. Belén von Baczko, Sección Paleontología de Vertebrados, Museo Argentino de Ciencias Naturales “Bernardino Rivadavia,” Av. Ángel Gallardo 470, C1405DJR, Ciudad Autónoma de Buenos Aires, Argentina. Email: belen_vb@macn.gov.ar

Funding information

Doris and Samuel Welles Grant; Fondo para la Investigación Científica y Tecnológica, Grant/Award Numbers: PICT 2016-159, PICT 2018-0717, PICT 2018-853; United States National Science Foundation, Grant/Award Numbers: IBN-0343744, IOB-0517257, IOS-1050154, IOS-1456503

Abstract

In the present contribution we revise, figure, and redescribe several isolated braincases of the iconic aetosaur *Desmotosuchus* from the *Placerias* Quarry locality, Chinle Formation, Arizona, United States. The detailed study of the isolated braincases from the UCMP collection allowed us to assign them at the species-level and recognize two species of *Desmotosuchus* for the *Placerias* Quarry: *D. spurensis* and *D. smalli*. The former can be distinguished from the latter by the presence of a transverse sulcus on the parietals, deep median pharyngeal recess on the basisphenoid, almost no gap between the basal tubera and the basiptyergoid processes, and the exoccipitals meeting at the midline. The presence of *D. smalli* at the *Placerias* Quarry has not been previously reported. Based on the braincases UCMP 27408, 27410, 27407, three new brain endocasts were developed through CT scan images, reconstructing the most complete endocranial casts known for an aetosaur, including the encephalon, cranial nerves, inner ear, and endocranial vasculature. The cranial endocasts also exhibited some differences between both species of *Desmotosuchus*, with *D. spurensis* having a distinguishable dural expansion and markedly asymmetric anterior and posterior semicircular canals of the labyrinth. Additionally, the combination of osteological features and the endocranial casts allowed us to identify and discuss the presence of an ossified orbitosphenoid on the anteriormost region of the braincase among aetosaurus. Furthermore, we were able to reinterpret some of the observations made by previous authors on the endocast of the holotype of *Desmotosuchus spurensis* (UMMP VP 7476) and provide some insight into their neurosensory capabilities.

KEYWORDS

aetosaurus, brain, Chinle Formation, paleoneurology, *Placerias* Quarry, Triassic

1 | INTRODUCTION

Aetosaurs are a monophyletic group of terrestrial, armored, quadrupedal pseudosuchian archosaurs known from Late Triassic continental outcrops. They are characterized by small, triangular skulls and a heavily ornamented articulated armor consisting of dorsal, lateral and, in some cases, ventral and appendicular osteoderms that covered their bodies (Desojo et al., 2013). This highly distinctive clade was distributed nearly worldwide (excepting Antarctica and Australia), but the majority of known species have been recovered from North America, where they are often the most common vertebrate element of their respective faunal assemblages (Long & Murry, 1995; Parker, 2007; Reyes et al., 2020). Aetosaurs traditionally have been regarded as the only herbivorous pseudosuchians (Walker, 1961; Small, 2002; Parker, 2007, 2018) within a primarily carnivorous archosaurian reptile fauna composed of rauisuchids, poposauroids, erpetosuchids, phytosaurs, crocodylomorphs, and dinosauriforms. However, other studies on aetosaurs have proposed a wider spectrum of feeding habits based on different qualitative and quantitative analysis (e.g., morphology, biomechanics, paleoneurology) (Desojo

et al., 2013; Desojo & Vizcaíno, 2009; Drózd, 2018; Small, 2002; Tabora et al., 2021).

The most emblematic aetosaur is *Desmatosuchus spurensis*, the largest known species, with characteristic lateral horns on its cervical osteoderms, an edentulous premaxilla, and serrated maxillary teeth with wear facets that are interpreted as reflecting herbivorous feeding habits (Figure 1a). A century ago, Case (1921) published the first description of an artificial physical cranial endocast for this species based on the holotype specimen (UMMP VP 7476) that had been prepared free of matrix, allowing him to begin exploring the systematic and paleobiological utility of paleoneuroanatomical information. Moreover, Case recognized that *Desmatosuchus spurensis* could be differentiated from phytosaurs based on their endocasts and cranial anatomy, reinforcing the idea that *Desmatosuchus* belonged to a different clade distinct from the Phytosauria (“Desmatosuchia: Desmatosuchidae” sensu Case, 1920, 1921). Edinger (1929) later discussed the endocast of *D. spurensis* based on Case’s work, including it in her landmark treatise on “fossil brains.” Subsequently, Hopson (1979) reevaluated this same specimen among a larger sample of

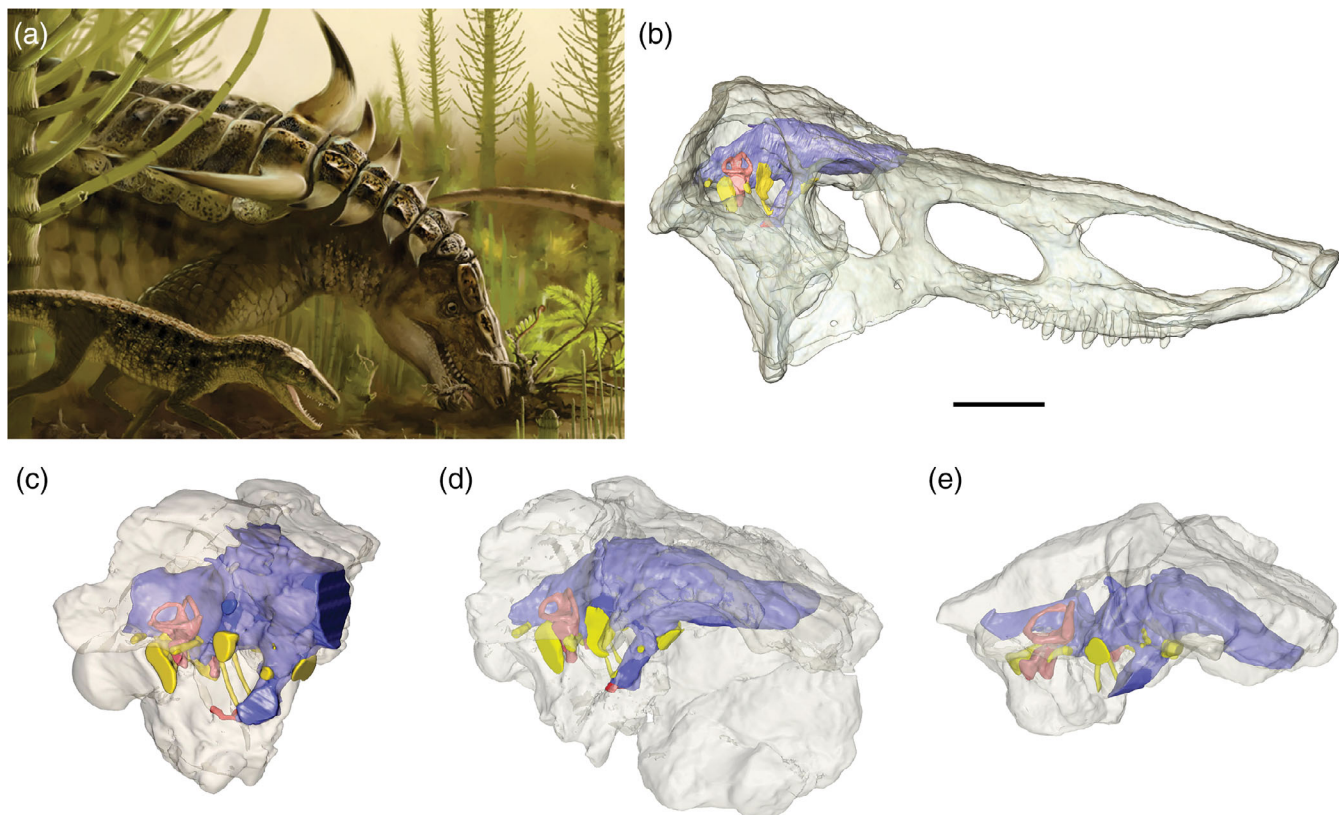


FIGURE 1 (a) Life reconstruction of *Desmatosuchus* (illustration by Victor Leshyk, taken from Desojo et al., 2013, Figure 9a); (b) semitransparent complete skull of *D. smalli* (cast TTUP 9024) with endocranial reconstruction of UCMP 27410 in place in lateral view; digital reconstruction of braincases (semitransparent) with endocasts of (c), UCMP 27408, (d), UCMP 27410; (e), UCMP 27407. Blue: encephalon; yellow: cranial nerves; pink: inner ear; red: internal carotids. Scale bar B equals 50 mm; (c)–(e) not to scale

endocranial casts in his review of reptile paleoneurology, and he provided alternative anatomical interpretations of some structures.

Since those seminal studies, paleoneurology has been recognized as a useful tool for paleobiological interpretations, because it can provide information about different biological aspects of extinct organisms, such as their locomotion, feeding habits, sensorial capacities, and behavior. Among extinct archosaurs, neuroanatomy has been extensively studied in Avemetatarsalia (i.e., stem-dinosaurs, dinosaurs, pterosaurs), but, despite some recent increased interest, pseudosuchian archosaurs have received less attention. Recent advances in pseudosuchian paleoneuroanatomy have included data on various major lineages, including Ornithosuchidae (*Riojasuchus tenuisiceps*; von Baczko & Desojo, 2016), Erpetosuchidae (*Parringtonia gracilis*; Nesbitt et al., 2017), Aetosauria (*Neoaetosauroides engaeus*; von Baczko et al., 2018), Loricata (*Prestosuchus chiniquensis*; Mastrantonio et al., 2019), and Phytosauria (Holloway et al., 2013; Lautenschlager & Butler, 2016; Lessner & Stocker, 2017). However, little is still known about endocranial diversity within most pseudosuchian lineages. In the particular case of aetosaurs, the braincase morphology of several species is reasonably well known, such as *Stagonolepis olenkae*, *Neoaetosauroides engaeus*, *Scutarx deltatylus*, *Longosuchus meadei*, *Desmatosuchus spurensis*, *D. smalli*, and *Aetosauroides scagliai* (Desojo & Báez, 2007; Gower & Walker, 2002; Paes Neto et al., 2021; Parker, 2005a, 2005b; Parker, 2016b; Parrish, 1994; Small, 2002; Sulej, 2010). Nonetheless, very few paleoneurological studies have been made on this clade, with the only published studies being the endocranial reconstructions of *Desmatosuchus spurensis* (Case, 1921) and *Neoaetosauroides engaeus* (von Baczko et al., 2018). The present contribution on the braincase endocast of *Desmatosuchus* allows us to expand paleoneurological knowledge on aetosaurs and to begin to document patterns in interspecific diversity within this group, as well as to evaluate aetosaurian diversity in the Late Triassic (Norian) *Placerias* Quarry (Chinle Formation, Arizona) and the implications for the biostratigraphic record for this locality.

1.1 | Institutional abbreviations

MACN-HE, Museo Argentino de Ciencias Naturales “Bernardino Rivadavia,” Colección Herpetología, Buenos Aires, Argentina; OUVC, Ohio University, Vertebrates Collection, Athens, United States; PEFO, Petrified Forest National Park, Arizona, United States; PVL, Instituto Miguel Lillo, Paleontología de Vertebrados, Tucumán, Argentina; TMM, Vertebrate Paleontology Collections, The University of Texas at Austin, Austin, United States;

TTUP, The Museum of Texas Tech University, Lubbock, United States; UCMP, University of California Museum of Paleontology, Berkeley, United States; UMMP, University of Michigan Museum of Paleontology, Ann Arbor, United States; ZPAL, Institute of Paleobiology, Polish Academy of Sciences, Warsaw, Poland.

2 | MATERIALS AND METHODS

Three specimens referable to *Desmatosuchus* collected from the *Placerias* Quarry (Upper Triassic, Chinle Formation, Apache County, Arizona, USA) were analyzed for this study—UCMP 27407, 27408, and 27410 (Figures 1 and 2). All three were studied firsthand and via CT scan data. Additionally, UMMP VP 7476 and several other specimens housed at the UCMP collection, Berkeley, United States, were studied firsthand for comparative purposes. The three UCMP specimens were scanned at OhioHealth O’Bleness Hospital (Athens, Ohio), using a General Electric (GE) LightSpeed Ultra Multislice CT scanner where they were scanned helically at a slice thickness of 625 μm , 120 kV, and 200 mA. UCMP 27408 was also scanned on a Bio-Imaging Research OMNI-X HD-600 industrial CT scanner at the Center for Quantitative Imaging at Penn State University (State College, Pennsylvania) at a slice thickness of 140 μm , 280 kV, and 2 mA. Scan data were imported into WitmerLab computer workstations, and the endocranial structures (brain endocast, inner ear labyrinth, vascular elements, etc.) were segmented using various versions of Amira/Avizo (Thermo Fisher Scientific, Waltham, MA). The 3D models were exported as OBJ files and imported into SimLab 3D Composer (Amman, Jordan) where 3D PDFs were generated. These 3D PDFs have been used to make the figures presented here.

CT data and 3D models are available at: <https://www.morphosource.org/projects/000382087>

As is typically the case with analyses of brain endocasts, we refer to regions of the brain, as well as to nerves, arteries, and veins in the endocasts using the same terms as their soft-tissue counterparts, but we recognize that the bony representations of these structures are not entirely faithful to the soft anatomy. The fidelity is particularly low for the brain itself, because the endocast also includes the volume occupied by other tissues surrounding the brain (i.e., meninges, vascular tissue), and, particularly in the case of reptiles (i.e., crocodylians, lepidosaurs, testudines) the brain clearly did not fill the endocranial cavity (Hopson, 1979; Paulina-Carabajal et al., 2014; Paulina-Carabajal & Currie, 2012; Witmer et al., 2008). The cephalic and pontine flexures of the endocasts were measured following the methods of

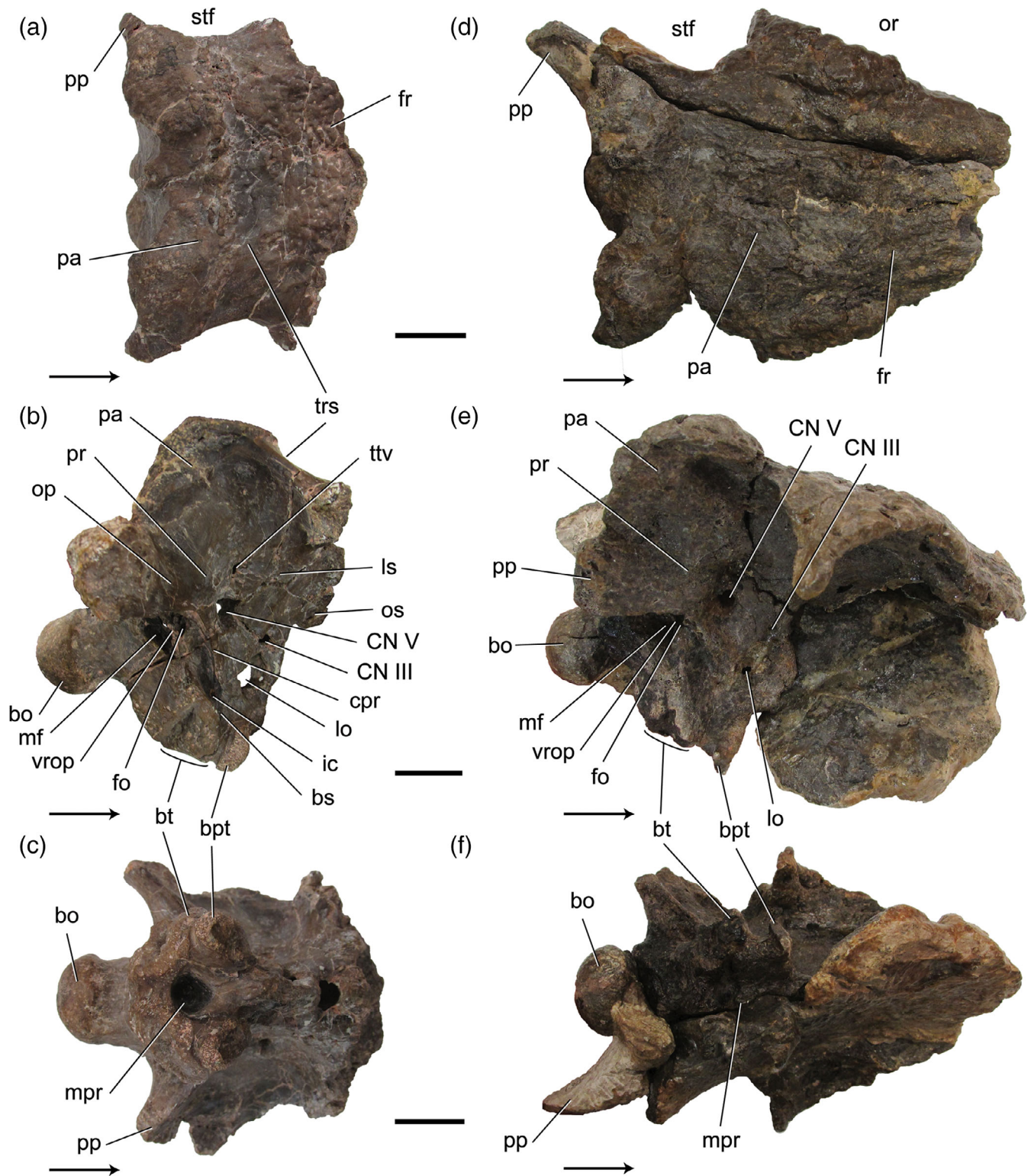


FIGURE 2 Brainscases of UCMP 27408 *Desmatosuchus spurensis* (a)–(c) and UCMP 27410 *Desmatosuchus smalli* (d)–(f) in dorsal, right lateral, and ventral views. bo, basioccipital; bpt, basipterygoid process; bs, basisphenoid; bt, basal tubera; CN, cranial nerve; cpr, crista prootica; fr, frontal; fo, fenestra ovalis; ic, cerebral branch of the internal carotid arteries; ls, laterosphenoid; lo, lateral opening; mf, metotic foramen; mpr, median pharyngeal recess; op, ophistic; or, orbit; os, orbitosphenoid; pa, parietal; pp, paroccipital process; pr, prootic; stf, supratemporal fenestra; trs, transverse sulcus; ttv, transversotrigeminal vein; vrop, ventral ramus of the ophistic. Scale bar equals 20 mm. Arrows indicate anterior direction

Lautenschlager and Hübner (2013). Measurements were calculated in the 3D models. The nomenclature for endocranial vasculature follows that of Early et al. (2020).

2.1 | Description and comparisons

The specimens of *Desmotosuchus* from the *Placerias* Quarry are exquisitely preserved generally, but their systematic assignment needed to be revised for different reasons. UCMP 27408 is a braincase with incomplete frontals (Figures 1c, 2a–c). It has been previously described and assigned to *Desmotosuchus haplocerus* by Small (1985, 2002), but more recent studies that reviewed the taxonomy of aetosaurs recognized *Desmotosuchus* (=“*Episcoposaurus*”) *haplocerus* as a *nomen dubium* (Parker, 2008, 2013, 2016a). As a consequence, Parker (2008) reassigned UCMP 27408 to *D. spurensis* because of the following similarities with the type specimen, UMMP VP 7476: presence of a transverse sulcus on the parietals, deep median pharyngeal recess on the basisphenoid, and almost no gap between the basal tubera and the basiptyergoid processes.

On the other hand, the unpublished specimen UCMP 27410 is a braincase with a complete skull roof, including part of the nasals (Figures 1d and 2d–f). The collection tag and UCMP catalogue identifies this specimen as either “*Desmotosuchus haplocerus*” or “*Desmotosuchus*” but no formal publication has properly justified this assignment. UCMP 27410 can be distinguished from the *D. spurensis* specimens UCMP 27408 and UMMP VP 7476 on the basis of the following: (a) absence of a transverse sulcus posteriorly delimited by a sharp edge on the dorsal surface of the parietals, having only a shallow depression on that region; (b) shallow median pharyngeal recess; (c) sizeable gap between the basal tubera and basiptyergoid processes; and (d) the exoccipitals not meeting at the midline. These features were recognized by Parker (2005a, 2005b) on the holotype and referred specimens of *D. smalli* (TTUP 9023, 9024, 9025, and 9420), and for that reason we assign UCMP 27410 to this species in the present contribution.

UCMP 27407 is a fragmentary and crushed braincase from the *Placerias* Quarry (digital reconstruction shown in Figure 1e) that was originally accessioned as “*Pseudosuchia*” but later informally identified on the specimen tag as “*Desmotosuchus haplocerus*.” It indeed does resemble *Desmotosuchus* in general terms, having tall parietals, a marked parietal protuberance for articulation with the osteoderms, and no postparietal fenestra. Unfortunately, the basal tubera and basiptyergoid processes are poorly preserved, and the depth of the medial pharyngeal recess cannot be reliably assessed. However, the exoccipitals do not appear to meet at the midline, and

there is no marked sulcus on the dorsal surface of the parietals. These last two characters would represent two of the (at least) four diagnostic cranial features noted by Parker (2005a, 2005b) for *D. smalli*. Thus, there is tentative justification for referring UCMP 27407 to *D. smalli*.

Although the aetosaur *Calyptosuchus wellsi* is also known from the *Placerias* Quarry, it is not possible to refer any of the three UCMP braincases under consideration here to that species because the holotype of *C. wellsi* has no cranial elements, and therefore there are no overlapping materials to compare. However, there are two braincases in the UCMP collections (UCMP 27414 and 27419) that differ from the morphology of *Desmotosuchus* according to Parker (2018), and perhaps a third one (UCMP 27409) which in turn might correspond to *C. wellsi* (Paes Neto et al., 2021). The morphology of these braincases differs from that of *Desmotosuchus* because the basiptyergoid processes are strongly projected anterolaterally with a well-delimited pit between these processes.

2.1.1 | General description of brain regions

The digital endocranial reconstructions presented here correspond primarily to UCMP 27408 (*Desmotosuchus spurensis*; Figure 3) and UCMP 27410 (*Desmotosuchus smalli*; Figure 4), with comments on the fragmentary UCMP 27407 provided when relevant (Figure 5). The reconstructed endocasts represent the encephalon, cranial nerves, inner ears, and several blood vessels. In general terms, the endocasts are sigmoidal in lateral view, tall, and have a similarly marked cephalic flexure of approximately 115–125° between the forebrain and midbrain, and a pontine flexure of 118–125° between midbrain and hindbrain. In the holotype of *D. spurensis*, the cephalic flexure is 110° and the pontine flexure 116°. In general, as with extant nonavian sauropsids and many Triassic archosaurs, there is likely a mismatch between the dural envelope of the brain (represented by the digital endocasts presented here) and the neural structure of the brain. As a result, many details of the brain itself are not apparent, and we will use the rough regional designations of fore-, mid-, and hindbrain as a means of organizing the descriptions.

The forebrain region is equally dominated by the cerebral hemispheres and olfactory tract and bulbs. The cerebral hemispheres are globose in all specimens, but they are barely laterally expanded compared to the rest of the encephalon. They are excavated on the ventral surface of the posterior region of the frontals and anterior region of the parietals and laterally enclosed by the laterosphenoids and ventrally by the orbitosphenoids.

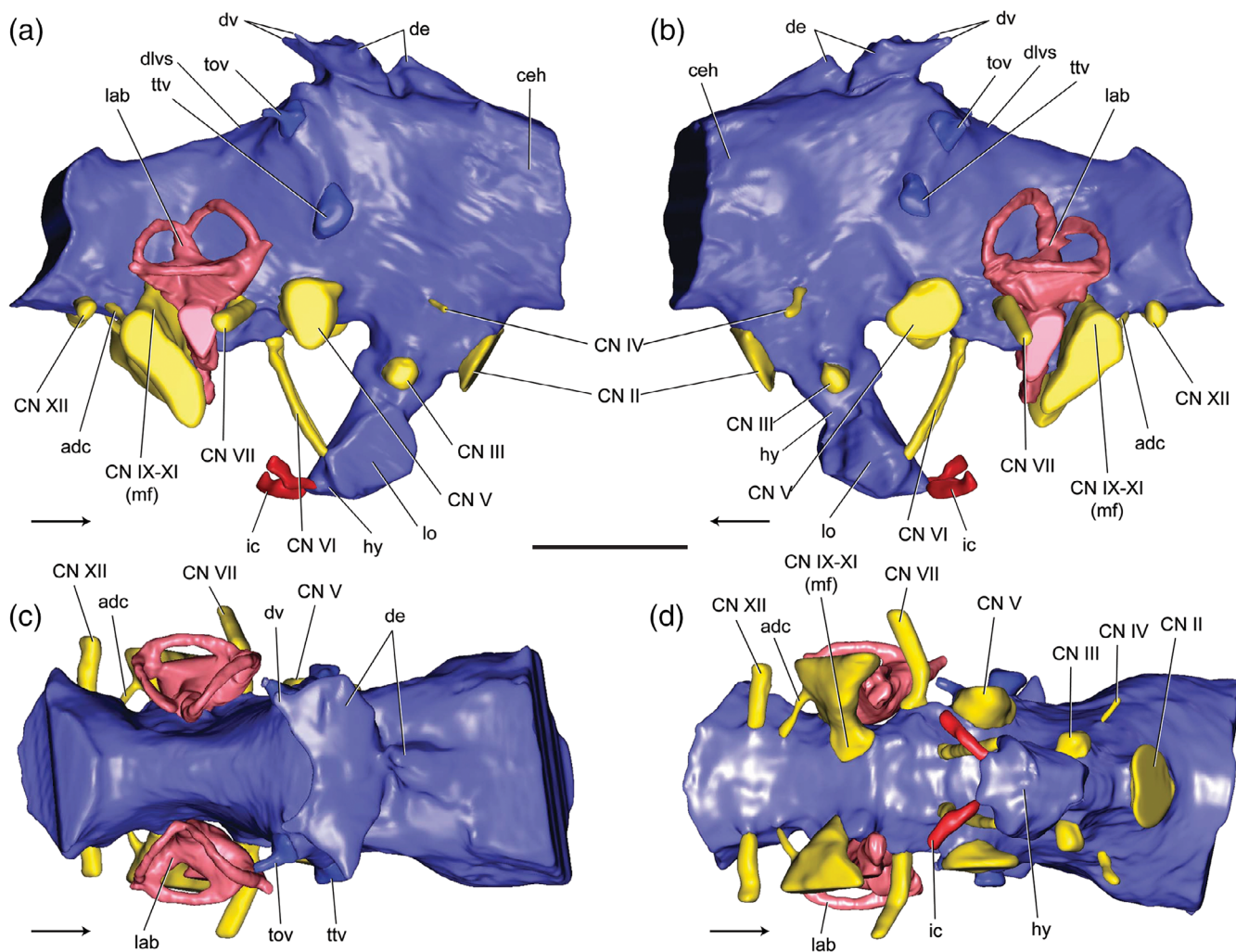


FIGURE 3 Digital endocasts of *Desmatosuchus spurensis* (UCMP 27408) in (a), right lateral, (b), left lateral, (c), dorsal, and (d), ventral views. adc, additional canal; ceh, cerebral hemispheres; CN, cranial nerve; de, dural expansion; dlvs, dorsal longitudinal venous sinus; dv, diploic vein; hy, hypophysis; ic, cerebral branch of the internal carotid arteries; lab, labyrinth; lo, lateral opening; mf, metotic foramen; tov, transversooccipital vein; ttv, transversotrigeminal nerve. Blue: encephalon; yellow: cranial nerves; pink: inner ear; red: internal carotids. Scale bar equals 20 mm. Arrows indicate anterior direction

The maximum width of the cerebral hemispheres is at the level of the postorbital crest (= *crista antotica*) of the laterosphenoids, but it is barely laterally expanded compared to its anterior portion (UCMP 27410) due to lack of any marked constriction in the region of the olfactory tracts (Figure 4c,d).

Large olfactory bulbs and tracts are excavated on the ventral surface of the frontals and are delimited post-erolaterally by laterosphenoids/orbitosphenoids (see Section 3). In life, the olfactory bulbs would be the targets for the olfactory neurons (cranial nerve I) and can be identified on the endocast of UCMP 27410 (*D. smalli*), but are not preserved in UCMP 27408 because the frontals are incomplete. The anterior margin of the olfactory bulbs of UCMP 27410 reaches the level of the anterior margin of the orbit (Figure 4). The bulbs in UCMP 27410

and the *D. spurensis* holotype (UMMP VP 7476) are approximately as long as wide, which is also the condition in other herbivorous archosaurs such as sauropod and ornithischian dinosaurs (e.g., *Diplodocus longus*: Witmer et al., 2008; *Hypacrosaurus altispinus*: Evans et al., 2009; *Euoplocephalus tutus*: Miyashita et al., 2011). The olfactory tracts are not distinct from the bulbs, lacking any constriction behind the two. The tracts are short and remarkably wide, being almost as wide as the cerebral hemispheres (UCMP 27410), which is a rare condition in archosaurs, being recognized only in other species of *Desmatosuchus* (e.g., *D. spurensis*: UMMP VP 7476).

The epiphysis (=pineal) is a dorsal diencephalic fore-brain structure whose status in the endocasts of *Desmatosuchus* is discussed further in the context of midline dorsal dural expansions (see Section 2.1.2). The

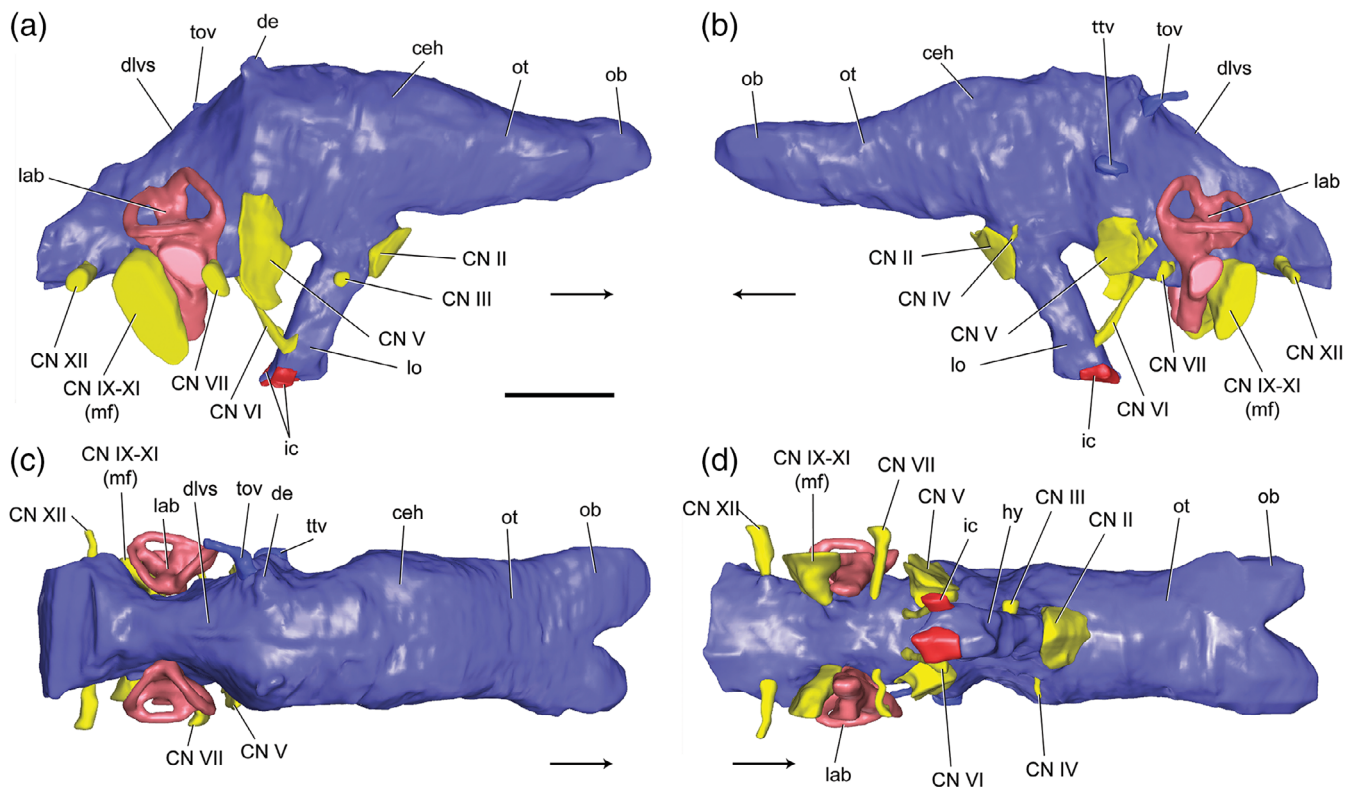


FIGURE 4 Digital endocast of *Desmatosuchus smalli* (UCMP 27410) in (a), right lateral, (b), left lateral, (c), dorsal, and (d), ventral views. ceh, cerebral hemispheres; CN, cranial nerve; de, dural expansion; dlvs, dorsal longitudinal venous sinus; hy, hypophysis; ic, cerebral branch of the internal carotid arteries; lab, labyrinth; lo, lateral opening; mf, metotic foramen; ob, olfactory bulb; ot, olfactory tract; tov, transversooccipital vein; ttv, transversotrigeminal nerve. Blue: encephalon; yellow: cranial nerves; pink: inner ear; red: internal carotids. Scale bar equals 20 mm. Arrows indicate anterior direction

hypophysis (=pituitary, formed in part by a diencephalic forebrain ventral expansion) in all three specimens (UCMP 27407, 27408, 27410) is posteroventrally directed when orienting the lateral semicircular canal of the labyrinth horizontally. This posteroventral angulation also characterizes the holotype of *Desmatosuchus spurensis* (UMMP VP 7476) and most archosaurs (e.g., *Alligator mississippiensis*, *Gavialis gangeticus*, *Sebecus icaeorhinus*: Hopson, 1979; *Simosuchus clarki*; Kley et al., 2010; *Carnotaurus sastrei*: Cerroni & Paulina-Carabajal, 2019, *Tyrannosaurus rex*, *Diplodocus longus*: Witmer et al., 2008; Witmer & Ridgely, 2009). However, this condition differs in phytosaurs (*Parasuchus angustifrons*, *Ebrachosuchus neukami*, *Smilosuchus gregorii*) and many ornithischians (*Corythosaurus* sp., *Hypacrosaurus altispinus*, *Arenysaurus ardevoli*) in which the hypophysis is ventrally directed when orienting the endocast with the same parameter (Cruzado-Caballero et al., 2015; Evans et al., 2009; Lautenschlager & Butler, 2016). As in other tetrapods, in these specimens of *Desmatosuchus* the deep hypophyseal cavity is located on the ventral surface of the forebrain, posterior to the foramen for the passage of the optic tracts (from here on “CN II”) and anterior to

the dorsum sellae. The lateral walls of the hypophyseal fossa exhibit two large openings in UCMP 27408 and UCMP 27410 (Figures 1 and 2) and the anterior wall is formed by the parabasisphenoid. In the type specimen of *D. spurensis* (UMMP VP 7476) both lateral openings are large and the anterior wall of the hypophyseal fossa is broken at its base. The braincase of UCMP 27407 is not sufficiently well preserved in this area to be certain whether these lateral apertures were present. In other aetosaurs the hypophyseal fossa is open anteriorly, as can be seen in *Neoaetosauroides engaeus* (PVL 5698), *Longosuchus meadei* (TMM 31185-84B), *Stagonolepis olenkae* (ZPAL AbIII/466/17), and *Scutarx deltatylus* (PEFO 34616).

The midbrain region, delimited approximately by the prootics, laterosphenoids, and parietals, does not show any clear evidence of mesencephalic structures such as the optic lobes. The expectation based on phylogenetic grounds is that the optic lobes would have contacted each other dorsally, separating the cerebrum from the cerebellum, as in extant crocodylians and other extant nonavian sauropsids (Hopson, 1979; Witmer et al., 2008). The absence of any optic lobe swellings that are discernable on the endocasts of UCMP 27408 and 27410 suggests that

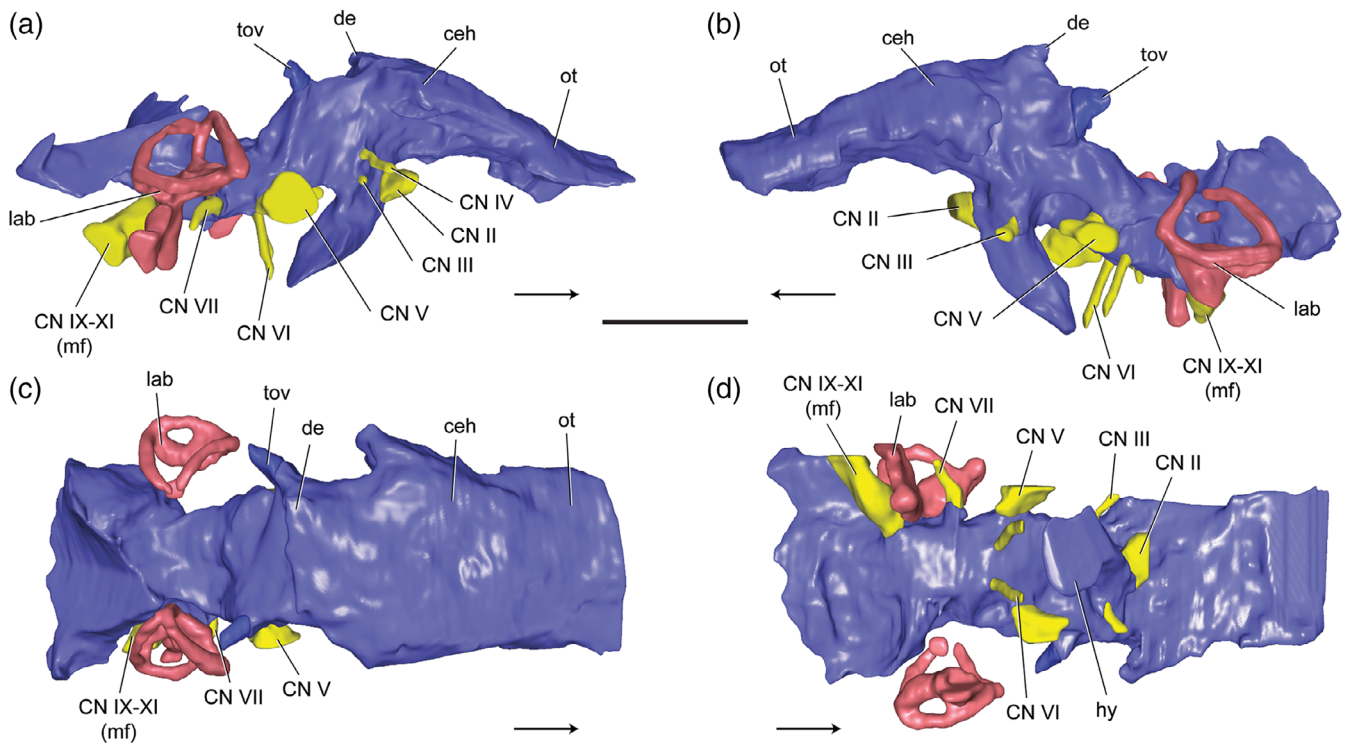


FIGURE 5 Digital endocast tentatively assigned to *Desmatosuchus smalli* (UCMP 27407) in (a), right lateral, (b), left lateral, (c), dorsal, and (d), ventral views. ceh, cerebral hemispheres; CN, cranial nerve; de, dural expansion; hy, hypophysis; lab, labyrinth; mf, metotic foramen; ot, olfactory tract; tov, transversooccipital vein. Blue: encephalon; yellow: cranial nerves; pink: inner ear; red: internal carotids. Scale bar equals 20 mm. Arrows indicate anterior direction

the neural structures of the midbrain tectum were modest in size at best. Therefore, the visual acuity might not have been remarkable in these animals and they were probably not particularly active (in concordance with the reduction of the floccular recess, see below).

The hindbrain region, delimited approximately by the parietals, supraoccipital, otoccipitals, prootics, and basioccipital, is also largely obscured, presumably by extensive dural venous sinuses. Given the constricted space between the endosseous labyrinths, the cerebellum must have been relatively modest in size. Likewise, the cerebellar expansion corresponding to the flocculus (=cerebellar auricle of fishes) must have been quite small, because the bony floccular recess is absent in UCMP 27408 and 27410.

2.1.2 | Endocranial vasculature

The endocasts of UCMP 27408 and 27410 have a noticeable swelling on their dorsal surface that corresponds to the dorsal longitudinal venous sinus, which runs along the dorsal surface of the brain and extends posteriorly (Figures 3 and 4). This region is poorly preserved in UCMP 27407 and the dorsal sinus cannot be clearly identified. A thick crest

running anteroventrally to posterodorsally can be clearly recognized on the lateral surface of the endocasts of UCMP 27407, 27408, and 27410. It separates the midbrain from the hindbrain and corresponds to the transverse dural venous sinus that runs along the tectal-otic sulcus between the laterosphenoid and prootic. This sinus exits the braincase through the foramen for the transversotrigeminal vein (=rostral/anterior middle cerebral vein), dorsal to the trigeminal foramen (Figures 3a,b, 4b,c), and the transversooccipital vein (=caudal/posterior middle cerebral vein) that can be identified on the dorsal end of this crest and pierces posterodorsally through the parietals, near their suture with the supraoccipital.

The dorsal portion of the endocast, slightly anterior to the transverse dural venous sinus, has features that could relate to either additional venous structures or the epiphysis (=pineal body) or both. The holotype (UMMP VP 7476) and referred (UCMP 27408) endocasts of *D. spurensis* both have a large tabular dural feature that projects posterodorsally (Figure 3). Case (1921) and Edinger (1929) regarded this feature as pertaining to the epiphysis, and this interpretation may well be correct. Indeed, the projection is consistent with this interpretation, being a midline structure between the cerebral hemispheres (forebrain) and optic lobes (midbrain). Hopson (1979), however, regarded

this feature as reflecting something like a fontanelle that would have been plugged with cartilage. This cartilage hypothesis was challenged (see Sampson & Witmer, 2007; Witmer et al., 2008), and the hypothesis that this dural expansion represents a “pineal peak” (Witmer et al., 2008) remains credible on both anatomical and phylogenetic grounds. That being said, the feature also has clear characteristics indicating a vascular—specifically a venous—origin. In particular, beyond its tabular shape, the structure (especially in UCMP 27408) has apices that are drawn out into sharp points. These pointed apices end in the substance of the bone and almost certainly represent diploic veins draining the substance of the bone. Such diploic veins draining into the dural venous sinus system are common in extant tetrapods and have been identified in other extinct archosaurs (sauropods: Witmer et al., 2008; Knoll et al., 2012; Sues et al., 2015; Martínez et al., 2016; theropods: Witmer & Ridgely, 2009). The interpretations of this median dorsal feature in the endocast as being associated with the dural venous sinus system and epiphysis are not in conflict, and both could be true. In extant diapsids with a clear pineal complex (e.g., birds, squamates, turtles), the epiphysis and its stalk project through the dural sinus space to reach the skull roof (Ghetie, 1976; Paulina-Carabajal et al., 2019).

Sulej (2010) identified a similar cavity in the skull roof of *Stagonolepis olenkae* (ZPAL Ab III/466/17, 504/1) that might be similar to the dural expansion noted here in *D. spurensis*. Sulej (2010) also regarded the cavity as housing a venous structure but regarded it as the dorsal head vein. The definitive dorsal head vein, however, if it opens at all into the endocranial cavity, typically passes through a foramen between the parietal, prootic, and otoccipital (Sampson & Witmer, 2007). There does not appear to be an endocranial aperture for the dorsal head vein in *Desmotosuchus*, and it is thus likely that the dorsal head vein (assuming it existed) anastomosed with the transversotrigeminal vein (=anterior middle cerebral vein), as proposed for the abelisaurid theropod *Majungasaurus* (Sampson & Witmer, 2007).

UCMP 27408 has another dural feature on the dorsal surface of the endocast, which takes the form of a short conical midline expansion (Figure 4: de). Based on its position, it would also be a candidate for the location of the epiphysis. However, in the holotype (UMMP VP 7476), the equivalent feature is split into a paired structure, which is not consistent with any part of the pineal complex (Quay, 1979). Indeed, Case (1921, p. 139) referred to these as “lateral processes,” whereas Edinger (1929, p. 123) referred to them as “problematic protuberances” (“problematische Protuberanzen”). Hopson (1979) again regarded them as remnants of persistent cartilage. Given their disposition in these two specimens, it is likely that they are simply additional dural expansions to receive diploic veins.

Interestingly, Sulej (2010) illustrated (but did not label) in *Stagonolepis olenkae* a median structure anterior to the larger dural expansion noted above that is similar to the structure in UCMP 27408. Perhaps surprisingly, the endocast of *Desmotosuchus smalli* (UCMP 27410) lacks the large median tabular dural expansion observed in the two endocasts of *D. spurensis* and probably *Stagonolepis olenkae*. UCMP 27410 does have a pair of dorsolateral dural processes that no doubt received diploic veins, but there are no prominent median features that would answer to a pineal peak, although there is a low swelling in this region. Without additional specimens, it is difficult to attribute this difference to individual variation or a species-level trait. For comparison, a sample of three endocasts of *Tyrannosaurus rex* was found to be overall quite similar but varied in the subtleties of various dural processes for diploic veins (Witmer & Ridgely, 2009). Nevertheless, the difference is consistent with other evidence arguing for two *Desmotosuchus* species in the Placerias Quarry. UCMP 27407 is the most damaged of the three UCMP braincases, and the crushing has impacted this region of the braincase. Although the transverse sinuses of UCMP 27407 are clear enough, the morphology of any dural expansions remains somewhat uncertain. There is some indication of the tabular dural expansion seen in endocasts of *D. spurensis* (UMMP VP 7476, UCMP 27408), even having some pointed apices to receive diploic veins, but deformation due to crushing makes these observations tentative. Otherwise, UCMP 27407 has no clear indication of a pineal peak.

The fossae and grooves surrounding the openings in the lateral walls of the hypophyseal cavity in UCMP 27408 and 27410 almost certainly transmitted vasculature, including modest sphenopalatine arteries and what must have been very large veins. The sphenopalatine arteries branched from the internal carotid arteries (Burda, 1969; Porter et al., 2016; Porter & Witmer, 2015; Sampson & Witmer, 2007; Sedlmayr, 2002), which, as described below, are very modest in size. As a result, most of the large lateral apertures in the hypophyseal cavity very likely transmitted large hypophyseal veins (Porter & Witmer, 2015) or orbital veins (Porter et al., 2016) from a large cavernous sinus (part of the endocranial dural venous sinus system) to what was likely a large lateral head vein. Thus, the hypophyseal structure indicated in the digital endocasts in Figures 3 and 4 housed a diversity of structures, including not only the hypophyseal (pituitary) gland itself but also arteries (internal carotid and sphenopalatine arteries) and veins (cavernous sinus, hypophyseal and/or orbital veins).

The cerebral branches of the internal carotid arteries can be identified entering the endocast posterolaterally on the distal end of the hypophysis of UCMP 27408 and 27410 (not preserved in UCMP 27407). The corresponding paired

openings can be seen in anterodorsal and anterolateral views of the braincase, at the base of the hypophyseal fossa and each can be traced to a foramen that opens on the lateral surface of the braincase, within the middle-ear space just behind the anteroventral end of the *crista prootica* (Figure 2b,e). This condition is typical of archosaurs but differs from the condition seen in many non-archosaurian archosauriforms (e.g., *Pseudochampsa ischigualastensis*, *Doswellia sixmilensis*, *Erythrosuchus africanus*, *Proterosuchus fergusi*) and erpetosuchid pseudosuchians (e.g., *Tarjadia ruthae*, *Parringtonia gracilis*) in which the cerebral branches of the internal carotid enter through a pair of foramina that open on the ventral surface of the parabasisphenoids (Dilkes & Sues, 2009; Ezcurra et al., 2017; Gower, 1996; Nesbitt et al., 2017; Trotteyn & Haro, 2012).

2.1.3 | Cranial nerves

A single exit for both optic tracts (“CN II”) can be recognized on the endocasts of both species, *Desmotosuchus spurensis* and *D. smalli*, and would correspond to the optic chiasm, prior to the divergence of the “CN II.” This exit is represented by a large opening located at the midline of the anteroventral surface of the braincases of UCMP 27407, 27408, and 27410 (Figures 3–5), anterior to the hypophysis and delimited by the orbitosphenoids and basisphenoid (see Section 3).

The passage for the oculomotor nerve (CN III) is larger than that of CN IV and can be identified at the suture between the laterosphenoid and orbitosphenoid, ventral to the postorbital ridge of the laterosphenoid, posterior to the opening for “CN II,” and dorsal to the lateral vascular openings of the hypophyseal fossa (Figure 2). It exits laterally on UCMP 27407, 27408, and 27410, near the base of the hypophyseal fossa at the level of the dorsum sellae (Figures 3a,b, 4a).

The exit for the trochlear nerve (CN IV) can be identified on UCMP 27407, 27408, and 27410 as a small passage on the anterior margin of the laterosphenoids (Figure 2b,e). The foramen cannot be clearly recognized on the exposed right side of UCMP 27410 (*Desmotosuchus smalli*) but its passage was identified on the left side through CT scan images (Figure 4b). On the other hand, the foramen for CN IV is easily recognized on both sides of UCMP 27408 (*Desmotosuchus spurensis*), anterior to the postorbital ridge of the laterosphenoid, at the contact of the orbitosphenoid and posterodorsal to the exit for “CN II” (Figure 3). The trochlear nerve projects anterolaterally with a slight ventral component in both species.

The trigeminal nerve (CN V) opening represents one of the largest foramina of the braincases of *Desmotosuchus*

(Figures 3–5). It has a single exit in UCMP 27407, 27408, and 27410, as well as UMMP VP 7476, which would imply that the CN V branches into its three rami outside the braincase as observed to occur in non-archosaurian archosauriforms (*Tropidosuchus romeri*: Trotteyn & Paulina-Carabajal, 2016; *Triopticus primus*: Stocker et al., 2016), sauropod and ornithischian dinosaurs, and pseudosuchians (e.g., *Wannia scurriensis*: Stocker et al., 2016; *Riojasuchus tenuisiceps*: PVL 3827; *Parringtonia fragilis*: Nesbitt et al., 2017; *Postosuchus kirkpatricki*: TTUP 9000, 9002; *Sebecus icaeorhinus*: Hopson, 1979; *C. yacare*: MACN-He 48841; *Alligator mississippiensis*: OUVC 9761). This condition differs from that of many but not all theropod dinosaurs and pterosaurs where the trigeminal nerve is inferred to have branched inside the braincase, with the ophthalmic ramus (V_1) exiting separately and more anteriorly to the maxillomandibular ramus ($V_{2,3}$) (Witmer et al., 2008). The main determinant of whether the trigeminal nerve rami diverge within the braincase (two or even three foramina) or outside of it (one foramen) is the location of the trigeminal (Gasserian) ganglion, which is the collection of cell bodies of the somatic sensory neurons that innervate rostrum and mandibles (Leitch & Catania, 2012; Sampson & Witmer, 2007; Witmer et al., 2008). *Desmotosuchus* is interpreted as sharing with other pseudosuchians (including extant crocodylians, although in these the trigeminal fossa is also delimited posteriorly by the quadrate) the plesiomorphic condition of having an extracranial position of the trigeminal ganglion, as probably suggested by an external fossa on the prootic and laterosphenoid bones of UCMP 27407, 27408, and especially UCMP 27410.

The section of the abducens nerve (CN VI) as reconstructed here is located on the ventral surface of the encephalon of UCMP 27407, 27408, and 27410, ventromedial to CN V (Figures 3–5); it projects anteroventrally reaching the posterolateral sides of the ventral end of the hypophysis, dorsal to the exits of the internal carotid arteries. In Case’s (1921) original description of the holotype endocast of *D. spurensis* (UMMP VP 7476), the ventral passages for CN VI were misinterpreted as the internal carotid arteries, but the exits for the carotid arteries are much more likely to be ventral to those for the abducens nerve, as also interpreted by Hopson (1979). CT scanning has allowed the entire abducens canal to be traced on both sides of each specimen, clarifying the identifications of previous authors based on physical endocasts.

The facial nerve (CN VII) projects laterally, exiting posterior to the dorsal margin of the *crista prootica* and anterior to the fenestra ovalis in UCMP 27407, 27408, and 27410 (Figures 2–5). This interpretation differs from that of Case (1921) for the holotype of *D. spurensis* (UMMP VP 7476). Case, followed by Edinger (1929),

identified a shared exit for CN VII and VIII that is dorso-laterally directed and located immediately next to the metotic foramen. However, this interpretation was probably influenced unduly by the nature of the physical endocast available to Case. Instead, as revealed by the digital endocasts of all three UCMP specimens, the dorsal passage very likely corresponds only to CN VIII, whereas the ventral one that exits laterally is CN VII. Both CN VII and VIII are located anterior to the constricted area of the encephalon where the inner ear would be located.

The metotic foramen transmits CN IX to XI and probably a large vein. In UCMP 27407, 27408, and 27410, it is located posterior to the fenestra ovalis, where it is bounded anteriorly by the ventral ramus of the ophistotic and posteriorly by the exoccipital component of the otoccipital (Figures 1, 3–5). The conformation of the metotic foramen is generally similar in the three UCMP endocasts, although UCMP 27408 has an unusual connection between the metotic foramen and brainstem region that is discussed further below along with the hypoglossal nerve. These digital endocasts allowed us to reinterpret the metotic foramen in the physical endocast of UMMP VP 7476, in which Case (1921) likely misinterpreted the exits for CN VII–XII. The passage for what Case interpreted as CN IX–XI is anterior to the inner ear and would not correspond to the metotic foramen but to the CN VII. We interpret the metotic foramen as being more posteriorly located, corresponding to what Case likely mistakenly interpreted as CN XII (Figure 6).

The hypoglossal nerve (CN XII) canal is similar in UCMP 27408 and 27410 (not adequately preserved in UCMP 27407), being a simple, transverse structure with a single aperture both internally and externally (Figures 3 and 4). In UCMP 27410 (*Desmotosuchus smalli*), this canal is the only candidate for the hypoglossal nerve. In UCMP 27408 (*Desmotosuchus spurensis*), however, there is an

additional internal foramen slightly anterior to the hypoglossal foramen that leads to a canal that passes antero-laterally to open externally within the deep fossa that is shared with the metotic foramen (Figure 3). The function of this canal may have different interpretations. If it transmitted a hypoglossal branch (e.g., XII₁), it would be exiting the braincase in a recess together with the metotic foramen, as in some crocodylians (*Gavialis gangeticus*, *Gryposuchus neogaeus*: Bona et al., 2017) and some dinosaurs (Knoll et al., 2015). Another possibility is that the canal transmitted a branch of the accessory nerve (CN XI), but such a course for the accessory nerve does not fit with the condition observed in living crocodylians and other diapsids where CN XI often exits the endocranium together with CN IX and X (=metotic foramen) (e.g., crocodylians, birds: von Wettstein, 1937-1954; most lizards: Székely & Matesz, 1988). The unusual canal is symmetrical in UCMP 27408, which shows no overt signs of pathology. It is not clear from the physical endocast of the holotype specimen of *D. spurensis* (UMMP VP 7476; Case, 1921) whether this unusual canal observed in UCMP 27408 was present, and thus resolution must await discovery of additional specimens. It is worth noting that having a single hypoglossal canal as in UCMP 27410 is also found in other aetosaurs such as *Neoaetosauroides engaeus* (von Baczko et al., 2018), *Stagonolepis olenkae* and *S. robertsoni* (Sulej, 2010), and cf. *Calypotosuchus* (UCMP 27409, 27414). *Paratypothorax andressorum* (Schoch & Desojo, 2016) also has a single external foramen for the CN XII but the number of internal openings cannot be determined. On the other hand, *Longosuchus meadei* (TMM 31185-84B) has two internal foramina aligned dorsoventrally and a single external foramen, which were not identified in the original description by Parrish (1994). The erpetosuchid *Parringtonia gracilis* has only one internal foramen for CN XII but two external foramina, and phytosaurs have a variable condition, some

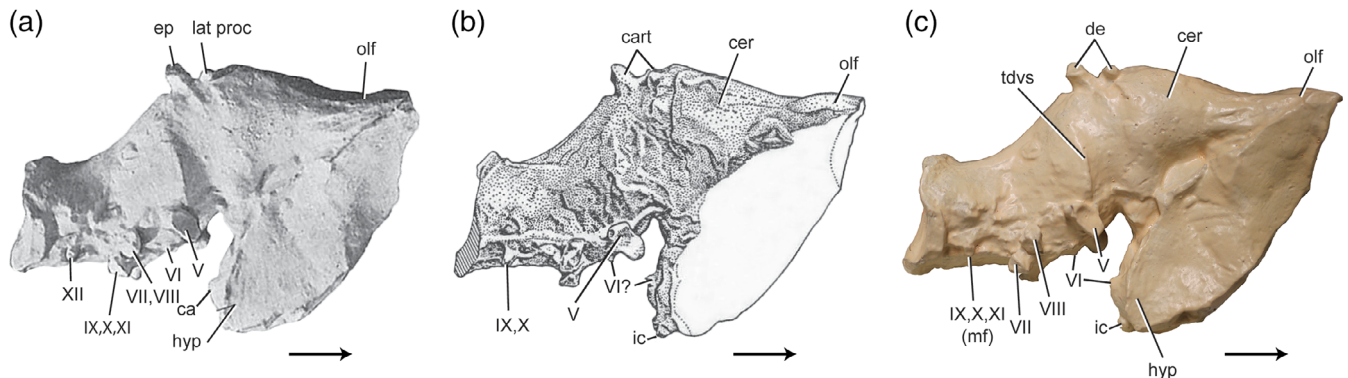


FIGURE 6 Comparisons of the interpretations of the artificial physical endocast of the holotype of *Desmotosuchus spurensis* (UMMP VP 7476). (a) Case, 1921 and (b) Hopson, 1979 (mirrored) with its original labels, (c) present study. ca/ic, internal carotid arteries; cer, cerebral hemispheres; de, dural expansion; ep, epiphysis; hyp, hypophysis; mf, metotic foramen; olf, olfactory bulb; lat proc, lateral process; tdvs, transverse dural venous sinus. Cranial nerves identified with their corresponding roman number. Arrows indicate anterior direction

having a single internal and external foramen for CN XII, such as *Parasuchus angustifrons* and *Ebrachosuchus neukami*, whereas others have double exits like *Parasuchus hislopi* (Hopson, 1979; Lautenschlager & Butler, 2016).

2.1.4 | Inner ear

The endosseous labyrinth of the inner ear of UCMP 27408 and 27410 (Figure 7) is completely preserved on both sides and on the right side of UCMP 27407, including the semicircular canals and the lagena (=cochlea of mammals). The inner ear of UCMP 27410 was previously illustrated by Stocker et al. (2016) but was not described. The semicircular canals in all three specimens are low, being twice anteroposteriorly wider as dorsoventrally high, as is the case in most non-archosaurian archosauriforms (e.g., *Chanaresuchus bonapartei*: Stocker et al., 2016; *Proterosuchus fergusi*: Brown et al., 2019; *Euparkeria capensis*: Sobral et al., 2016) and pseudosuchians (e.g., phytosaurs: Holloway et al., 2013; Lautenschlager & Butler, 2016; Lessner & Stocker, 2017; *Parringtonia gracilis*: Nesbitt

et al., 2017; *Gracilisuchus stipanicorum*: Stocker et al., 2016; semiaquatic crocodylomorphs: Schwab et al., 2020). This contrasts with the aetosaur *Neoaetosauroides engaeus* (von Baczko et al., 2018), the rauisuchid *Postosuchus* sp. (Stocker et al., 2016), and theropod and sauropod dinosaurs (e.g., *Carnotaurus sastrei*: Cerro & Paulina-Carabajal, 2019; *Majungasaurus crenatissimus*: Sampson & Witmer, 2007; *Tyrannosaurus rex*, *Diplodocus longus*: Witmer et al., 2008) in which the labyrinth is approximately as wide as high.

The strongly convex curvature of the anterior semicircular canal (ASC) is larger (radius of curvature) than the curvature of the posterior semicircular canal (PSC). This difference is more noticeable in UCMP 27408 (*D. spurensis*), the ASC being twice as large as the PSC, whereas in UCMP 27410 (*D. smalli*) it is 1.5 times larger (Figure 7). This asymmetric condition between ASC and PSC contrasts with that of *Neoaetosauroides engaeus*, the only other aetosaur with a described cranial endocast, in which the curvature of the ASC is subequal to the PSC (von Baczko et al., 2018). The curvatures of ASC and PSC are more subequal in UCMP 27407, but this condition is likely due to distortion caused

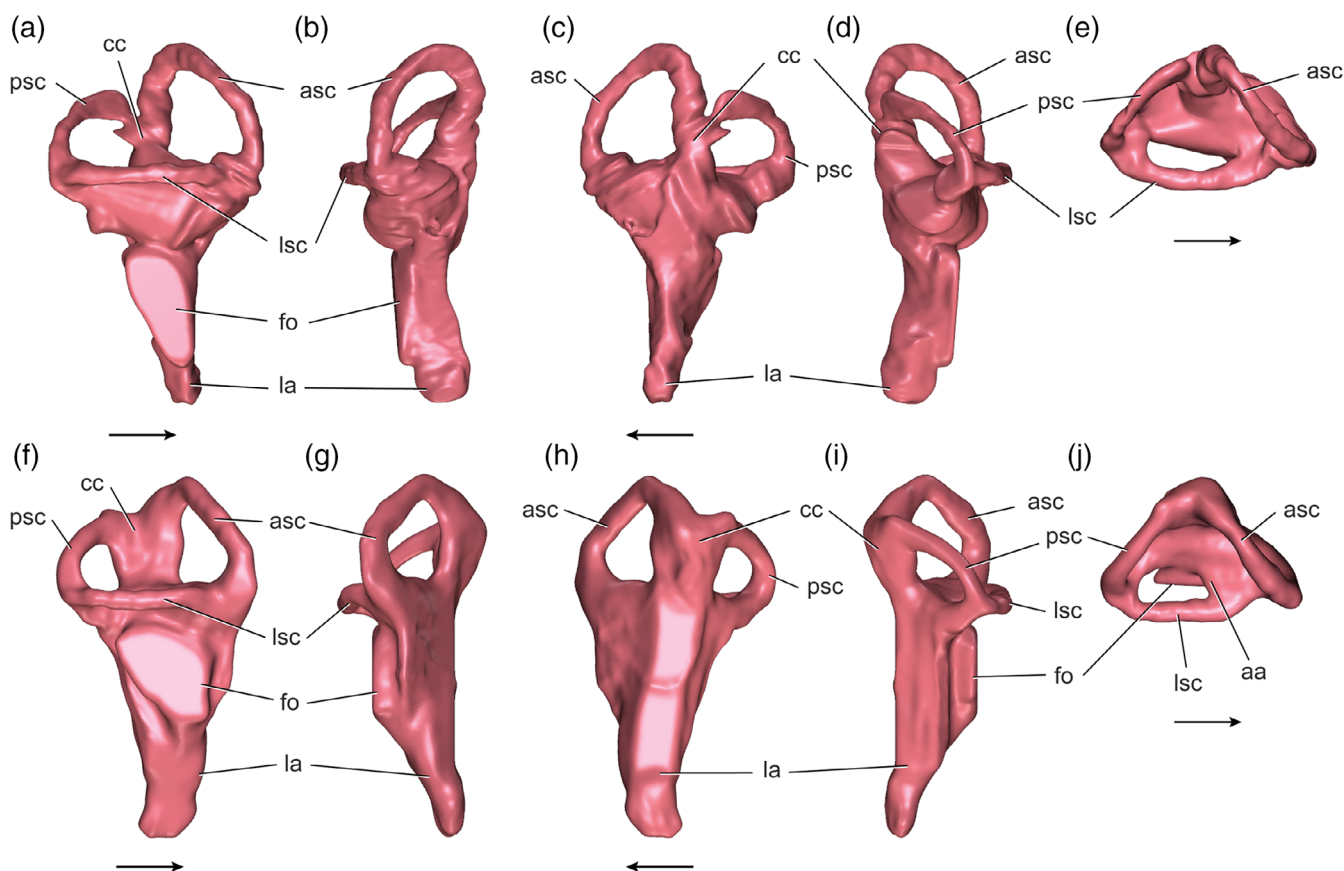


FIGURE 7 Right inner ear of UCMP 27408 (*Desmatosuchus spurensis*) in (a), lateral, (b), anterior, (c), medial, (d), posterior, and (e), dorsal views. Left inner ear (mirrored) of UCMP 27410 (*Desmatosuchus smalli*) in (f), lateral, (g) anterior, (h), medial, (i), posterior, and (j), dorsal views. aa, anterior ampulla; asc, anterior semicircular canal; cc, common crus; fo, fenestra ovalis; la, lagena; lsc, lateral semicircular canal; psc, posterior semicircular canal. Arrows indicate anterior direction

by crushing. The angle formed in dorsal view between the ASC and PSC of UCMP 27407, 27408, and 27410 is less than 90° as in some other archosauriforms, including *Neoaetosauroides engaeus*, *Parringtonia gracilis*, *Triopticus primus*, but differing from that in phytosaurs (e.g., *Machaeropsopus mccauleyi*, Holloway et al., 2013; *Wannia scurriensis*, Lessner & Stocker, 2017; *Parasuchus angustifrons*, *Ebrachosuchus neukami*, Lautenschlager & Butler, 2016), *Euparkeria capensis* (Sobral et al., 2016), *Chanaresuchus bonapartei* (Stocker et al., 2016), *Proterosuchus fergusi* (Brown et al., 2019), *Gracilisuchus stipanicorum* (Stocker et al., 2016), *Postosuchus* cf. *kirkpatricki* (Stocker et al., 2016), and crocodylomorphs (*Caiman yacare*: MACN-HE 48841; *Alligator mississippiensis*: OUVC 9761; *Gavialis gangeticus*, *Gryposuchus neogaeus*: Bona et al., 2017) in which it is approximately 90°. The shape of the lateral semicircular canal (LSC) seen in dorsal view shows some differences between the two species of *Desmotosuchus*, being convex in UCMP 27407 (*D. smalli*) and UCMP 27408 (*D. spurensis*) but straight in UCMP 27410 (*D. smalli*) and with a very large anterior ampulla on the latter.

The representation of the hearing organ (lagena/cochlea) in an endocast is regarded as the portion ventral to the fenestra ovalis and thus depends partly on the conformation of the latter. For example, the fenestra ovalis is relatively tall dorsoventrally in UCMP 27408, resulting in a relatively short lagena, whereas in UCMP 27410, the fenestra ovalis is shorter, resulting in a longer lagena (Figure 7). The archosauriforms *Triopticus primus* and *Proterosuchus fergusi* and the pseudosuchians *Parringtonia gracilis*, *Gryposuchus neogaeus*, *Alligator mississippiensis*, and *Gavialis gangeticus* also have short lagenae that do not exceed the height of the labyrinth (Bona et al., 2017; Brown et al., 2019; Nesbitt et al., 2017; Stocker et al., 2016).

In UCMP 27408 (*D. spurensis*) the fenestra ovalis is taller than wide, as in *Alligator mississippiensis* (OUVC 9761), contrasting with the lower and more rounded ones of UCMP 27410 (*D. smalli*) (Figure 7a,f), phytosaurs (*Parasuchus angustifrons*, *Ebrachosuchus neukami*, *Wannia scurriensis*), *Parringtonia gracilis*, and *Triopticus primus* (Lautenschlager & Butler, 2016; Lessner & Stocker, 2017; Nesbitt et al., 2017; Stocker et al., 2016).

3 | DISCUSSION AND CONCLUSION

3.1 | Presence of the orbitosphenoid in aetosaurs

We recognize the presence of ossified orbitosphenoids in *Desmotosuchus*, because the foramen for CN III is

completely enclosed by bone. According to embryological information in extant crocodylians, this foramen is posteriorly delimited by the *pila antotica*, which ossifies into the laterosphenoids (Clark et al., 1993; Werneburg & Yaryhin, 2018), and anteriorly delimited by the *pila metoptica*, which forms the cartilaginous orbitosphenoids but do not ossify (Bellairs & Kamal, 1981; Clark et al., 1993; Liem et al., 2001). For this reason, in extant crocodylians, the anterior border of the foramen for CN III is open and represented only by a notch on the anterior margin of the laterosphenoid. On the other hand, in extant crocodylians the foramen for CN IV is located on the anterior margin of the laterosphenoid but is usually completely enclosed by this element in adults, whereas in dinosaurs and extant birds it is delimited by the orbitosphenoid and laterosphenoid. Moreover, there are few apparent sutures between the areas that would correspond to these two elements at the lateral walls of the braincase of *Desmotosuchus* (UCMP 27408, 27410).

Based on this evidence we propose two hypotheses: (a) according to our observations in extant crocodylians, the ossified area anterior to the foramen for CN III would correspond to the orbitosphenoid, which is restricted to the ventral part of the anterior region of the braincase, it encloses “CN II” but does not touch the skull roof and (b) based on the evidence of dinosaurs (including extant birds), the anterior margin of the foramina for CN III and IV is formed by the orbitosphenoid. In the first scenario, the laterosphenoid would be inserted between the orbitosphenoid and the frontal (Figure 8a). Following the second hypothesis, the orbitosphenoid of *Desmotosuchus* would be higher and might reach the skull roof (i.e., frontal), with the laterosphenoid located posterior to it (Figure 8b).

The foramina for “CN II” and III have also been identified in other aetosaurs such as *Stagonolepis olenkae* (Sulej, 2010), *Desmotosuchus smalli* (Small, 2002), and *Longosuchus meadei* (Parrish, 1994) but the elements that shape them have been debated. Parrish (1994) recognized the presence of the orbitosphenoid on the anteriormost part of the braincase of *Longosuchus*, which would be delimiting “CN II” and anterior margin of CN III in TMM 31185-84B, but Gower and Walker (2002) suggested that it corresponds to the anterior process of the laterosphenoid after their revision of the braincase of *Stagonolepis robertsoni*. The latter interpretation was then followed by Small (2002) and Sulej (2010) in their descriptions of *Desmotosuchus “haplocerus”* (in which Small combined specimens of *D. spurensis* and *D. smalli* as these were then considered the same species) and *Stagonolepis olenkae*, respectively. Both authors interpreted an anteroposteriorly elongate laterosphenoid enclosing the foramen for “CN II” and forming the anterior margin of the foramen for CN III

in both species. However, on the braincase of UCMP 27408 (*D. spurensis*) and UCMP 27410 (*D. smalli*), the presence of the foramina for CN III and IV helped clarify the identity of the anteriormost element of the braincase as the orbitosphenoid, supporting the proposal of Parrish (1994).

3.2 | Analysis of previous interpretations for *Desmotosuchus spurensis*

The neuroanatomy of *Desmotosuchus spurensis* was originally described by Case (1921) based on an artificial physical endocast of the holotype UMMP VP 7476, and a few modifications were mentioned or illustrated by Edinger (1929), who largely accepted Case's identifications, as well as Hopson (1979), who offered some alternatives. For instance, Case misidentified the passage of the cerebral branch of the internal carotids (Figure 6a), whereas Hopson (1979) rectified this error, locating them at the ventralmost end of the hypophyseal fossa (Figure 6b). The passage located dorsal to the cerebral branch of the internal carotids was suggested by the latter author as the ventral passage of CN VI, which connects to the dorsal exit of this nerve at the base of the encephalon (already identified by Case). The CT scan data for

UCMP 27408 allows us to corroborate the exit for CN VI at the base of the encephalon as originally proposed by Case and its ventral passage near the hypophysis as suggested by Hopson (1979). Moreover, our digital endocasts of UCMP 27408 and 27410 support Hopson's interpretation of the position of the cerebral branch of the internal carotids.

Case (1921) identified the exit for CN XII at the posteriormost region of the endocast of UMMP VP 7476, but Hopson (1979) mentioned that the same large foramen corresponded to CN IX–X. Our digital endocast UCMP 27408 allowed us to identify the foramina for CN XII as well as the metotic foramen, for CN IX–XI, located posterior to the constricted region of the encephalon where the inner ear fits. This constriction also can be seen on the endocast of UMMP VP 7476 and allowed us to identify the exit for CN IX–XI together posterior to the endosseous labyrinth, rejecting Case's interpretation about CN IX–XII. Additionally, we agree with Hopson on the position of CN IX and X but incorporate CN XI to the same exit (Figure 6c).

Case (1921) also identified the exit for CN VII and VIII together, located dorsal to what he identified as a common exit for CN IX–XI, in UMMP VP 7476. According to our results, these CNs are positioned

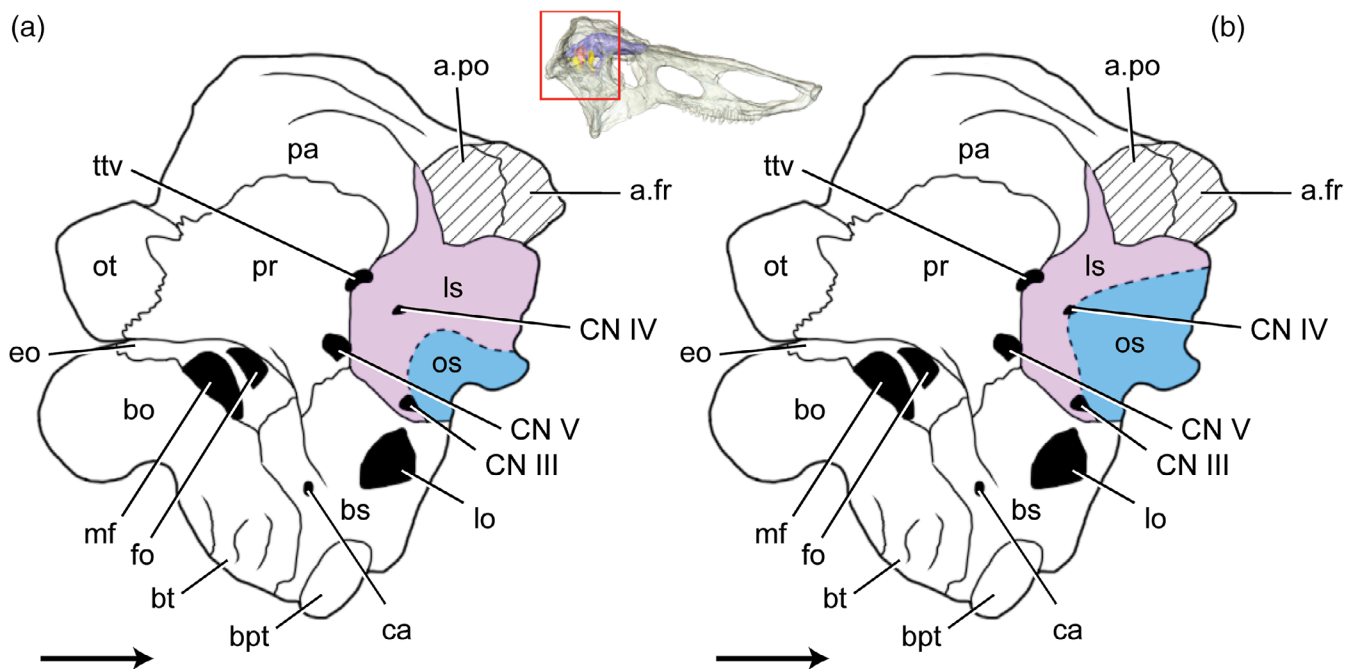


FIGURE 8 Schematic of the braincase of *Desmotosuchus* showing the presence and extension of the ossified orbitosphenoid. (a) Hypothesis based on evidence from extant crocodylians, (b) hypothesis based on evidence from non-avian dinosaurs and extant birds. a. fr, articulation for the frontal; a.po, articulation for the postorbital; bo, basioccipital; bs, basisphenoid; bt, basal tubera; bpt, basipterygoid process; CN, cranial nerve; eo, exoccipital; fo, fenestra ovalis; ca, cerebral branch of the internal carotid arteries; ls, laterosphenoid; lo, lateral opening; mf, metotic foramen; os, orbitosphenoid; ot, otoccipital; pa, parietal; pr, prootic; ttv, transversotrigeminal vein. Arrows indicate anterior direction

anterior to the endosseous labyrinth, and for that reason the exit for the CN IX–XI cannot be as Case (1921) indicated. The latter would actually correspond to the foramen for CN VII, as in UCMP 27408, and therefore the foramen located dorsal to this one would be restricted to that for CN VIII (Figure 6c).

3.3 | New materials of *Desmotosuchus* from the UCMP collections

After the analysis of UCMP 27408 and 27410, which allowed us to identify these isolated braincases to species level (*Desmotosuchus spurensis* and *D. smalli*, respectively), we were able to assign at least five additional specimens to both species of *Desmotosuchus* based exclusively on neurocranial features.

Desmotosuchus spurensis is characterized by the presence of a deep transverse sulcus on the parietals, the exoccipitals contacting at the midline, a deep medial pharyngeal recess, and the absence of a gap between basal tubera and basiptyergoid processes (following Parker, 2005a, 2005b, 2008). The two following isolated braincases from the UCMP collection can be referred to *D. spurensis* in addition to UCMP 27408: UCMP 27417 and 27420.

Desmotosuchus smalli is differentiated by having parietals without a transverse sulcus (only a slight depression on that region), a shallow medial pharyngeal recess that is confluent anteriorly with a depressed area that fades at the level of the basiptyergoid processes, a sizeable gap between basal tubera and basiptyergoid processes, and exoccipitals that do not meet at the midline (following Parker, 2005a, 2005b; Paes Neto et al., 2021). Along with UCMP 27410, the isolated braincases UCMP 27418, 27421, and 27345 can be referred to *D. smalli*.

Additionally, we tentatively refer the specimen UCMP 27407 to *Desmotosuchus smalli* based on the absence of the transverse sulcus on the parietal and the exoccipitals not meeting at the midline. The information provided by the cranial endocast also might support this assignment because the anterior and posterior semicircular canals show a similar proportion to those observed in UCMP 27410 (*D. smalli*), and the dorsal region of the endocast lacks the short conical dural expansion on the midline seen in UCMP 27408 therefore differing from *D. spurensis*.

3.4 | Systematic Paleontology

Archosauria Cope, 1869 sensu Gauthier and Padian, 1985
 Pseudosuchia Zittel, 1887–1890 sensu Gauthier and Padian, 1985
 Aetosauria Marsh, 1884 sensu Parker, 2007

Stagonolepididae Lydekker, 1887 sensu Walker, 1961
 Desmotosuchinae Huene, 1942 sensu Heckert & Lucas, 2000

Desmotosuchini Parker, 2016a

Desmotosuchus Case, 1920

Desmotosuchus spurensis Case, 1920

Holotype. UMMP VP 7476, skull, nearly complete dermal armor, articulated cervical and dorsal vertebral column, ilium.

Type Locality. East bank of Blanco River, about a half mile east of the old mail road from Spur to Crosbyton, Crosby County, Texas. Tecovas Formation, Dockum Group, early Norian.

Referred specimens. MNA V9300, posterior portion of right mandible, fragmentary dentary, almost complete vertebral column, complete pelvis, and majority of the dermal armor; UCMP 27408, isolated braincase; UCMP 27417, basioccipital and basisphenoid; 27420, partial braincase.

Desmotosuchus smalli Parker, 2005a

Holotype. TTUP 9024, nearly complete skull and right mandible, partial pelvis, femora, nearly complete cervical armor and numerous plates from the rest of the dermal armor (Parker, 2005a).

Type Locality. Post (Miller) Quarry, nine miles southeast of Post, Garza County, Texas, United States. Cooper Canyon Formation, Dockum Group, Norian.

Paratypes. TTUP 9023, well-preserved skull including braincase and mandibles, scapulocoracoid, humerus, a single dorsal vertebra, lateral cervical spine, assorted dorsal armor; TTUP 9025, partial skull including teeth; TTUP 9170, right humerus and ulna; TTUP 9027, pelvis.

Referred specimens. DMNH 1160-8, lateral osteoderm spike; DMNH 9889, osteoderm fragments; DMNH 9890, anterior caudal vertebrae; DMNH 9893, partial paramedian osteoderm with complete lateral edge; DMNH 9906, incomplete anterior caudal vertebra; DMNH 9909, incomplete lateral osteoderm horn; DMNH 9910, nearly complete lateral osteoderm horn; DMNH 9913, caudal vertebra; DMNH 9939, extremely large partial sacrum; DMNH 9940, several fragmentary paramedian osteoderms and fragment of a lateral osteoderm; DMNH 9941, nearly complete paramedian osteoderm; DMNH 9998, incomplete lateral osteoderm horn; TTUP 09023, excellent skull missing the snout, scapulocoracoid, humerus, a single dorsal vertebra, lateral cervical spine, assorted dorsal armor; TTUP 09025, partial skull; TTUP 09204, extensive but mostly fragmentary osteoderms, ribs, probable interclavicles; TTUP 09207, incomplete skull; TTUP 09225, proximal end of humerus; TTUP 09226, four incomplete lateral osteoderms and two rib fragments; TTUP 09229, well-preserved paramedian osteoderms and numerous osteoderm fragments; TTUP 09416 (in part), good cervical,

dorsal, and caudal vertebrae, and an well-preserved scapulocoracoid; TTUP 09419, vertebrae and appendicular material including a partial pelvis, fragmentary osteoderms; TTUP 09420 (in part), mostly disarticulated skull, several cervical vertebrae and lateral osteoderms; TTUP 10083, right humerus and ulna, incomplete lateral osteoderm; UCMP 27410, braincase; UCMP 27418, basioccipital and parabasisphenoid; UCMP 27421, basioccipital, exoccipitals, and parabasisphenoid; UCMP 27345, incomplete braincase.

Several aetosaurs have been recognized from the *Placerias* Quarry (“*Stagonolepis*” *wellesi*, *Desmatosuchus* “*haplocerus*,” *Acaenasuchus* *geoffreyi*) by previous authors (e.g., Irmis, 2005; Long & Murry, 1995; Parker, 2005a, 2005b), primarily by Long and Murry (1995) who carried out most of the identifications. These were posteriorly reevaluated by Parker (2005b, 2008, 2018) who identified other aetosaur taxa and only recognized *Desmatosuchus spurensis* and *Calyptosuchus wellsi* as valid species. Our results increase the aetosaur diversity of the *Placerias* Quarry in the Sonsela Member, Chinle Formation, providing a new record of the species *Desmatosuchus smalli* at this locality.

Desmatosuchus smalli was previously recorded from the Martha's Butte beds of the Sonsela Member, Chinle Fm., Arizona, and the Cooper Canyon Fm., Dockum Group, Texas (Martz et al., 2013; Parker, 2016a), which would correspond to a Norian age (Ramezani et al., 2014). *Desmatosuchus smalli* was originally identified from the Post Quarry, western Texas, forming one of the most diverse aetosaur assemblages known to date. According to our results, its novel presence in the *Placerias* Quarry bolsters previous statements that the diversity of the *Placerias* Quarry would be comparable or equivalent to that of the Post Quarry (Irmis, 2005; Long & Murry, 1995; Martz et al., 2013; Parker, 2005b). The new additional specimens of *D. spurensis* and *D. smalli* do not represent a change to the biostratigraphic record for the Upper Triassic of North America (e.g., Parker, 2018), but would suggest a coeval occurrence for these species.

Based on previous biostratigraphic works on the *Placerias* Quarry vertebrate assemblage, most authors have referred *Desmatosuchus* specimens exclusively to *D. “haplocerus”* and overlooked the presence of other *Desmatosuchus* species at that time. This might be a consequence of assigning specimens mainly based on osteoderm morphology and that none of the osteoderms found so far at this locality present the apomorphies of *D. smalli* (Parker, 2005a, 2005b). For this reason, and in light of the new information, the taxonomic assignment of the UCMP specimens mentioned in previous publications (Heckert & Lucas, 2000; Long & Murry, 1995; Parker, 2005b, 2008, 2018) should continue to be reevaluated. For example, the comparisons with the

endosseous labyrinth of *Desmatosuchus spurensis* UCMP 27410 provided by von Baczko et al. (2018) actually correspond to *Desmatosuchus smalli*.

3.5 | Paleobiological inferences

Some neuroanatomical features from the endocasts of *Desmatosuchus spurensis* and *Desmatosuchus smalli* provide some insight into their neurosensory capabilities and ultimately their habits. As previously mentioned, the large and rounded olfactory bulbs of *Desmatosuchus* suggest an emphasis on sensing odors in their environment. They resemble the olfactory bulbs of some other herbivorous archosaurs (e.g., many sauropod and ornithischian dinosaurs), contrasting with the elongated and narrow bulbs of the aetosaur *Neoaetosauroides engaeus* (von Baczko et al., 2018) and most pseudosuchians (i.e., phytosaurs, erpetosuchids, gracilisuchids, basal loricatans), which were likely animalivores. These associations may suggest reliance among herbivores on olfactory cues (perhaps arising from the vegetation) beyond those pertaining to sensing conspecifics and potential predators. Based on these findings, a logical next step would be a quantitative analysis of the olfactory apparatus incorporating not just dinosaurs (where most of the effort has been spent thus far) but also pseudosuchians.

The absence of optic lobe swellings on the endocasts of both species of *Desmatosuchus*, combined with the modest size of their orbits, suggests that their visual sense might have been unremarkable, although the discovery of scleral ossicles would help refine our assessments of the visual system because scleral rings provide the best quantitative estimates from the skeleton of such optically important parameters as dimensions of the eyeball, lens, and pupil (Cerio & Witmer, 2020; Choiniere et al., 2021; Hall, 2008, 2009; Schmitz, 2009). This information, combined with the small size of the floccular recess and the moderate size of the semicircular canals of the labyrinth, would suggest that highly coordinated gaze stabilization mechanisms were not present, and that, by extension, these species of *Desmatosuchus* were probably not especially active or agile animals. This also would be in concordance with the large and heavy body structure of *Desmatosuchus*, which could reach up to 5–6 m in length and 280 kg of body mass (Desojo et al., 2013; Kubo & Benton, 2007; Parker, 2008). Their voluminous bodies were also entirely covered by a heavy spiked dermal armor which might have further restricted their agility (e.g., fused cervical osteoderms and elongated cervical spines restrict flexion of the neck in *D. spurensis*).

Edinger (1942) associated a well-developed hypophysis (pituitary) with large body sizes in extinct archosaurs,

and likewise, Kamilar and Tecot (2015) related large hypophyseal size with rapid pre- and postnatal growth rates in mammals. In the case of *Desmotosuchus*, the large hypophysis seen in the studied specimens, UCMP 27408, 27410, 27407, as well as the holotype UMMP VP 7476, are consistent with both proposals because *Desmotosuchus* could reach very large body sizes and a rapid growth rate was previously inferred through histological studies (de Ricqlès et al., 2003).

Some other aspects of endocranial anatomy are more difficult to interpret from a functional standpoint. For example, there are clear differences in the structure of the dural expansions on the dorsal aspect of the endocast between *Desmotosuchus spurensis* (UCMP 27408) and *D. smalli* (UCMP 27410). Differences in the form of the dural expansions has been explored in sauropods (Witmer et al., 2008) and tyrannosaurids (Witmer & Ridgely, 2009), and there is wide agreement that these structures represent elements of the dural venous sinus system. However, no obvious functional implications for the differences are apparent, and few testable hypotheses have been offered (Case, 1921; Edinger, 1929; Hopson, 1979; Sampson & Witmer, 2007). Nevertheless, as the sample of endocasts increases and the diversity of these structures is documented, it is hoped that interpretable patterns will emerge.

ACKNOWLEDGMENTS

We thank Voltaire Paes Neto, Ariana Paulina-Carabajal, and William Parker for their suggestions and comments during the early development of the manuscript. For assistance with CT scanning, we thank Heather Rockhold and OhioHealth O'Bleness Hospital, Athens, Ohio, and Avrami Grader and Tim Ryan at the Center for Quantitative Imaging, Pennsylvania State University. For help in collections and access to and loan of specimens, we thank J. Howard Hutchison, Patricia A. Holroyd, and Kevin Padian (UCMP), and the late Gregg Gunnell (UMMP). We thank the reviewers, William Parker and Michelle Stocker, as well as the editors, Casey Holliday and Emma Schachner, for their comments and suggestions that helped improve the quality of the manuscript.

AUTHOR CONTRIBUTIONS

Maria Belen von Baczko: Conceptualization-Equal, Funding acquisition-Equal, Investigation-Equal, Methodology-Equal, Project administration-Equal, Resources-Equal, Supervision-Equal, Validation-Equal, Visualization-Equal, Writing-original draft-Equal, Writing-review & editing-Equal. **Julia Desojo:** Conceptualization (equal); funding acquisition (equal); investigation (equal); methodology (equal); project administration (equal); resources (equal); visualization (equal); writing – original draft (equal); writing


– review and editing (equal). **David Gower:** Conceptualization (equal); investigation (equal); methodology (equal); resources (equal); writing – review and editing (equal). **Ryan Ridgely:** Funding acquisition (equal); methodology (equal); resources (equal); software (equal). **Paula Bona:** Funding acquisition (equal); investigation (equal); methodology (equal); writing – review and editing (equal). **Lawrence Witmer:** Funding acquisition (equal); investigation (equal); methodology (equal); resources (equal); software (equal); supervision (equal); writing – original draft (equal); writing – review and editing (equal).

ORCID

M. Belén von Baczko  <https://orcid.org/0000-0003-2570-3418>

Julia B. Desojo  <https://orcid.org/0000-0002-2739-3276>

Paula Bona  <https://orcid.org/0000-0001-7782-855X>

Lawrence M. Witmer  <https://orcid.org/0000-0002-7610-0118>

REFERENCES

- Bellairs, A. A., & Kamal, A. M. (1981). The chondrocranium and the development of the skull in recent reptiles. In C. Gans & T. S. Parsons (Eds.), *Biology of the Reptilia* (pp. 11:1–11:263). Academic Press.
- Bona, P., Paulina-Carabajal, A., & Gasparini, Z. (2017). Neuroanatomy of *Gryposuchus neogaeus* (Crocodylia, Gavialoidea): A first integral description of the braincase and endocranial morphological variation in extinct and extant gavialoids. *Earth and Environmental Science Transactions of the Royal Society of Edinburgh*, 106, 235–246.
- Brown, E. E., Butler, R. J., Ezcurra, M. D., Bhullar, B. A. S., & Lautenschlager, S. (2019). Endocranial anatomy and life habits of the Early Triassic archosauriform *Proterosuchus fergusi*. *Palaeontology*, 63, 255–282.
- Burda, D. J. (1969). Developmental aspects of intracranial arterial supply in the alligator brain. *The Journal of Comparative Neurology*, 135, 369–380.
- Case, E. C. (1921). On an endocranial cast from a reptile, *Desmotosuchus spurensis*, from the Upper Triassic of western Texas. *The Journal of Comparative Neurology*, 33, 132–147.
- Case, E. C. (1920). Preliminary description of a new suborder of phytosaurian reptiles with a description of a new species of Phytosaurus. *The Journal of Geology*, 28, 524–535.
- Cerio, D. G., & Witmer, L. M. (2020). Modeling visual fields using virtual ophthalmoscopy: Incorporating geometrical optics, morphometrics, and 3D visualization to validate an interdisciplinary technique. *Vision Research*, 167, 70–86.
- Cerroni, M. A., & Paulina-Carabajal, A. (2019). Novel information on the endocranial morphology of the abelisaurid theropod *Carnotaurus sastrei*. *Comptes Rendus Palevol*, 18, 985–995.
- Choiniere, J. N., Neenan, J. M., Schmitz, L., Ford, D. P., Chappelle, K. E., Balanoff, A. M., Sipla, J. S., Georgi, J. A., Walsh, S. A., Norell, M. A., Xu, X., Clark, J. M., & Benson, R. B. J. (2021). Evolution of vision and hearing modalities in theropod dinosaurs. *Science*, 372, 610–613.

- Clark, J. M., Welman, J., Gauthier, J. A., & Parrish, J. M. (1993). The laterosphenoid bone of early archosauriforms. *Journal of Vertebrate Paleontology*, 13, 48–57.
- Cruzado-Caballero, P., Fortuny, J., Llacer, S., & Canudo, J. I. (2015). Paleoneuroanatomy of the European lambeosaurine dinosaur *Arenysaurus ardevoli*. *PeerJ*, 3, e802.
- de Ricqlès, A. J., Padian, K., & Horner, J. R. (2003). On the bone histology of some Triassic pseudosuchian archosaurs and related taxa. *Annales de Paléontologie*, 89, 67–101.
- Desojo, J. B., & Báez, A. M. (2007). Cranial morphology of the Late Triassic South American archosaur *Neoaetosauroides engaeus*: Evidence for aetosaurian diversity. *Palaeontology*, 50, 267–276.
- Desojo, J. B., Heckert, A. B., Martz, J. W., Parker, W. G., Schoch, R. R., Small, B. J., & Sulej, T. (2013). Aetosauria: A clade of armoured pseudosuchians from the Upper Triassic continental beds. In S. J. Nesbitt, J. B. Desojo, & R. B. Irmis (Eds.), (Vol. 379, pp. 203–239). Geological Society, . Special Publications.
- Desojo, J. B., & Vizcaíno, S. F. (2009). Jaw biomechanics in the South American aetosaur *Neoaetosauroides engaeus*. *Paläontologische Zeitschrift*, 83, 499–510. <https://doi.org/10.1007/s12542-009-0032-6>
- Dilkes, D., & Sues, H. D. (2009). Redescription and phylogenetic relationships of *Doswellia kaltenbachi* (Diapsida: Archosauriformes) from the Upper Triassic of Virginia. *Journal of Vertebrate Paleontology*, 29, 58–79.
- Drózd, D. (2018). Osteology of a forelimb of an aetosaur *Stagonolepis olenkae* (Archosauria: Pseudosuchia: Aetosauria) from the Krasiejów locality in Poland and its probable adaptations for a scratch-digging behavior. *PeerJ*, 6, e5595. <https://doi.org/10.7717/peerj.5595>
- Early, C. M., Iwaniuk, A. N., Ridgely, R. C., & Witmer, L. M. (2020). Endocast structures are reliable proxies for the sizes of corresponding regions of the brain in extant birds. *Journal of Anatomy*, 237, 1162–1176.
- Edinger, T. (1929). Die fossilen Gehirne. *Ergebnisse der Anatomie und Entwicklungsgeschichte*, 28, 1–249.
- Edinger, T. (1942). The pituitary body in giant animals fossil and living: A survey and a suggestion. *The Quarterly Review of Biology*, 17(1), 31–45.
- Evans, D. C., Ridgely, R., & Witmer, L. M. (2009). Endocranial anatomy of lambeosaurine hadrosaurids (Dinosauria: Ornithischia): A sensorineural perspective on cranial crest function. *The Anatomical Record*, 292, 1315–1337.
- Ezcurra, M. D., Fiorelli, L. E., Martinelli, A. G., Rocher, S., Baczko, M. B., Ezpeleta, M., Taborda, J. R. A., Hechenleitner, E. M., Trotteyn, M. J., & Desojo, J. B. (2017). Deep faunistic turnovers preceded the rise of dinosaurs in southwestern Pangaea. *Nature Ecology and Evolution*, 1, 1477–1483.
- Ghetie, V. (1976). *Atlas de anatomie a pasarilor domestice [Anatomical atlas of domestic birds]* (pp. 1–294). Editura Academiei Republicii Socialiste Romaniaa.
- Gower, D. J. (1996). The braincase of the early archosaurian reptile *Erythrosuchus africanus*. *Journal of Zoology*, 242, 557–576.
- Gower, D. J., & Walker, A. D. (2002). New data on the braincase of the aetosaurian archosaur (Reptilia: Diapsida) *Stagonolepis robertsoni* Agassiz. *Zoological Journal of the Linnean Society*, 136, 7–23.
- Hall, M. I. (2008). The anatomical relationships between the avian eye, orbit and sclerotic ring: Implications for inferring activity patterns in extinct birds. *Journal of Anatomy*, 212(6), 781–794.
- Hall, M. I. (2009). The relationship between the lizard eye and associated bony features: A cautionary note for interpreting fossil activity patterns. *The Anatomical Record*, 292(6), 798–812.
- Heckert, A. B., & Lucas, S. G. (2000). Taxonomy, phylogeny, biostratigraphy, biochronology, paleobiogeography, and evolution of the Late Triassic Aetosauria (Archosauria: Crurotarsi). *Zentralblatt für Geologie und Paläontologie, Teil I*, 1998(11–12), 1539–1587.
- Holloway, W. L., Claeson, K. M., & O’Keefe, F. R. (2013). A virtual phytosaur endocast and its implications for sensory system evolution in archosaurs. *Journal of Vertebrate Paleontology*, 33, 848–857.
- Hopson, J. A. (1979). Paleoneurology. In C. Gans, R. Northcutt, & P. Ullinski (Eds.), *Biology of the reptilia* (pp. 39–146). Academic Press.
- Irmis, R. (2005). The vertebrate fauna of the Upper Triassic Chinle Formation in Northern Arizona. Guidebook to the Triassic Formations of the Colorado Plateau in northern Arizona: Geology, Paleontology, and History. In S. J. Nesbitt, W. G. Parker, & R. B. Irmis (Eds.), *Mesa Southwest Museum, Bulletin No. 9*. Southwest Paleontological Society.
- Kamilar, J. M., & Tecot, S. R. (2015). Connecting proximate mechanisms and evolutionary patterns: Pituitary gland size and mammalian life history. *Journal of Evolutionary Biology*, 28, 1997–2008.
- Kley, N. J., Sertich, J. J., Turner, A. H., Krause, D. W., O’Connor, P. M., & Georgi, J. A. (2010). Craniofacial morphology of *Simosuchus clarki* (Crocodyliformes: Notosuchia) from the late Cretaceous of Madagascar. *Journal of Vertebrate Paleontology*, 30(Supp. 1), 13–98.
- Knoll, F., Witmer, L. M., Ortega, F., Ridgely, R. C., & Schwarz-Wings, D. (2012). The braincase of the basal sauropod dinosaur *Spinophorosaurus* and 3D reconstructions of the cranial endocast and inner ear. *PLoS One*, 7, e30060.
- Knoll, F., Witmer, L. M., Ridgely, R. C., Ortega, F., & Sanz, J. L. (2015). A new titanosaurian braincase from the Cretaceous “Lo Hueco” locality in Spain sheds light on neuroanatomical evolution within Titanosauria. *PLoS One*, 10, e0138233.
- Kubo, T., & Benton, M. J. (2007). Evolution of hindlimb posture in archosaurs: Limb stresses in extinct vertebrates. *Palaeontology*, 50(6), 1519–1529.
- Lautenschlager, S., & Butler, R. J. (2016). Neural and endocranial anatomy of Triassic phytosaurian reptiles and convergence with fossil and modern crocodylians. *PeerJ*, 4, e2251.
- Lautenschlager, S., & Hübner, T. (2013). Ontogenetic trajectories in the ornithischian endocranium. *Journal of Evolutionary Biology*, 26, 2044–2050.
- Leitch, D. B., & Catania, K. C. (2012). Structure, innervation, and response properties of integumentary sensory organs in crocodylians. *Journal of Experimental Biology*, 215, 4217–4230.
- Lessner, E. J., & Stocker, M. R. (2017). Archosauriform endocranial morphology and osteological evidence for semiaquatic sensory adaptations in phytosaurs. *Journal of Anatomy*, 231, 655–664.
- Liem, K., Bemis, W., Walker, W., & Grande, L. (2001). *Functional anatomy of the vertebrates. An evolutionary perspective* (3rd ed.). Harcourt College Publishers.
- Long, R. A., & Murry, P. A. (1995). Late Triassic (Carnian and Norian) tetrapods from the southwestern United States. *New Mexico Museum of Natural History & Science Bulletin*, 4, 1–254.

- Martínez, R. D. F., Lamanna, M. C., Novas, F. E., Ridgely, R. C., Casal, G. A., Martínez, J., Vita, J. R., & Witmer, L. M. (2016). A basal lithostrotian titanosaur (Dinosauria: Sauropoda) with a complete skull: Implications for the evolution and paleobiology of Titanosauria. *PLoS One*, *11*, e0151661.
- Martz, J. W., Mueller, B., Nesbitt, S. J., Stocker, M. R., Parker, W. G., Atanassov, M., Fraser, N., Weinbaum, J., & Lehane, J. R. (2013). A taxonomic and biostratigraphic re-evaluation of the Post Quarry vertebrate assemblage from the Cooper Canyon Formation (Dockum Group, Upper Triassic) of southern Garza County, western Texas. *Earth and Environmental Science Transactions of the Royal Society of Edinburgh*, *103*, 339–364.
- Mastrantonio, B. M., von Baczko, M. B., Desojo, J. B., & Schultz, C. L. (2019). The skull anatomy and cranial endocast of the pseudosuchid archosaur *Prestosuchus chiniquensis* from the Triassic of Brazil. *Acta Palaeontologica Polonica*, *64*, 171–198.
- Miyashita, T., Arbour, V. M., Witmer, L. M., & Currie, P. J. (2011). The internal cranial morphology of an armoured dinosaur *Euoplocephalus* corroborated by X-ray computed tomographic reconstruction. *Journal of Anatomy*, *219*, 661–675.
- Nesbitt, S. J., Stocker, M. R., Parker, W. G., Wood, T. A., Sidor, C. A., & Angielczyk, K. D. (2017). The braincase and endocast of *Parringtonia gracilis*, a Middle Triassic suchian (Archosaur: Pseudosuchia). *Journal of Vertebrate Paleontology*, *37*, 122–141.
- Paes Neto, V., Desojo, J. B., Brust, A. C. B., Ribeiro, A. M., Schultz, C. L., & Soares, M. B. (2021). The first braincase of the basal aetosaur *Aetosauroides scagliai* (Archosauria: Pseudosuchia) from the Upper Triassic of Brazil. *Journal of Vertebrate Paleontology*, *41*(2), e1928681.
- Parker, W. G. (2005a). A new species of the Late Triassic aetosaur *Desmotosuchus* (Archosauria: Pseudosuchia). *Comptes rendus de l'Académie des Sciences*, *4*, 327–340.
- Parker, W. G. (2005b). Faunal review of the Upper Triassic Chinle Formation of Arizona. *Mesa Southwest Museum Bulletin*, *11*, 34–54.
- Parker, W. G. (2007). Reassessment of the aetosaur “*Desmotosuchus*” *chamaensis* with a reanalysis of the phylogeny of the Aetosauria (Archosauria: Pseudosuchia). *Journal of Systematic Palaeontology*, *5*, 41–68.
- Parker, W. G. (2008). Description of new material of the aetosaur *Desmotosuchus spurensis* (Archosauria: Suchia) from the Chinle Formation of Arizona and a revision of the genus *Desmotosuchus*. *PaleoBios*, *28*, 1–40.
- Parker, W. G. (2013). Redescription and taxonomic status of specimens of *Episcoposaurus* and *Typhorax*, the earliest known aetosaurs (Archosauria: Suchia) from the Upper Triassic of western North America, and the problem of proxy “holotypes”. *Earth and Environmental Science Transactions of the Royal Society of Edinburgh*, *103*, 313–338.
- Parker, W. G. (2016a). Revised phylogenetic analysis of the Aetosauria (Archosauria: Pseudosuchia); assessing the effects of incongruent morphological character sets. *PeerJ*, *4*, e1583.
- Parker, W. G. (2016b). Osteology of the Late Triassic aetosaur *Scutarx deltatylus* (Archosauria: Pseudosuchia). *PeerJ*, *4*, e2411.
- Parker, W. G. (2018). Redescription of *Calyptosuchus* (*Stagonolepis*) *wellesi* (Archosauria: Pseudosuchia: Aetosauria) from the Late Triassic of the Southwestern United States with a discussion of genera in vertebrate paleontology. *PeerJ*, *6*, e4291.
- Parrish, J. M. (1994). Cranial osteology of *Longosuchus meadei* and the phylogeny and distribution of the Aetosauria. *Journal of Vertebrate Paleontology*, *14*, 196–209.
- Paulina-Carabajal, A., Carballido, J. L., & Currie, P. J. (2014). Braincase, neuroanatomy, and neck posture of *Amargasaurus cazaui* (Sauropoda, Dicraeosauridae) and its implications for understanding head posture in sauropods. *Journal of Vertebrate Paleontology*, *34*, 870–882.
- Paulina-Carabajal, A., & Currie, P. J. (2012). New information on the braincase of *Sinraptor dongi* (Theropoda: Allosauroidea): Ethmoidal region, endocranial anatomy, and pneumaticity. *Vertebrata Palasiatica*, *4*, 85101.
- Paulina-Carabajal, A., Sterli, J., & Werneburg, I. (2019). The endocranial anatomy of the stem turtle *Naomichelys speciosa* from the Early Cretaceous of North America. *Acta Palaeontologica Polonica*, *64*, 711–716.
- Porter, W. R., Sedlmayr, J. C., & Witmer, L. M. (2016). Vascular patterns in the heads of crocodylians: Blood vessels and sites of thermal exchange. *Journal of Anatomy*, *229*, 1–25.
- Porter, W. R., & Witmer, L. M. (2015). Vascular patterns in iguanas and other squamates: Blood vessels and sites of thermal exchange. *PLoS One*, *10*, e0139215.
- Quay, W. B. (1979). The parietal eye–pineal complex. In C. Gans, R. G. Northcutt, & P. Ulinski (Eds.), *Biology of the Reptilia (Neurology A)* (pp. 245–406). Academic Press.
- Ramezani, J., Fastovsky, D. E., & Bowring, S. A. (2014). Revised chronostratigraphy of the lower Chinle Formation strata in Arizona and New Mexico (USA): High-precision U–Pb geochronological constraints on the Late Triassic evolution of dinosaurs. *American Journal of Science*, *314*, 981–1008.
- Reyes, W. A., Parker, W. G., & Marsh, A. D. (2020). Cranial anatomy and dentition of the aetosaur *Typhorax coccinarum* (Archosauria: Pseudosuchia) from the Upper Triassic (Revuelian–mid Norian) Chinle Formation of Arizona. *Journal of Vertebrate Paleontology*, *40*(6), e1876080.
- Sampson, S. D., & Witmer, L. M. (2007). Craniofacial anatomy of *Majungasaurus crenatissimus* (Theropoda: Abelisauridae) from the Late Cretaceous of Madagascar. *Memoirs of the Society of Vertebrate Paleontology* 8. *Journal of Vertebrate Paleontology*, *27*(Suppl. 2), 32–102.
- Schmitz, L. (2009). Quantitative estimates of visual performance features in fossil birds. *Journal of Morphology*, *270*, 759–773.
- Schoch, R. R., & Desojo, J. B. (2016). Cranial anatomy of the aetosaur *Paratyphorax andressorum* Long & Ballew, 1985, from the Upper Triassic of Germany and its bearing on aetosaur phylogeny. *Neues Jahrbuch für Geologie und Paläontologie-Abhandlungen*, *279*, 73–95.
- Schwab, J. A., Young, M. T., Neenan, J. M., Walsh, S. A., Witmer, L. M., Herrera, Y., Allain, R., Brochu, C. A., Choiniere, J. N., Clark, J. M., Dollman, K. N., Etches, S., Fritsch, G., Gignac, P. M., Ruebenstahl, A., Sachs, S., Turner, A. H., Vignaud, P., Wilberg, E. W., ... Brusatte, S. L. (2020). Inner ear sensory system changes as extinct crocodylomorphs transitioned from land to water. *Proceedings of the National Academy of Sciences of the United States of America*, *117*, 10422–10428.
- Sedlmayr, J. C. (2002). *Anatomy, evolution, and functional significance of cephalic vasculature in Archosauria* (Doctoral dissertation). Ohio University.

- Small, B. J. (1985). *The Triassic thecodontian reptile Desmatosuchus: Osteology and relationships* (MSc thesis). Texas Tech University (pp. 1–97).
- Small, B. J. (2002). Cranial anatomy of *Desmatosuchus haplocerus* (Reptilia: Archosauria: Stagonolepididae). *Zoological Journal of the Linnean Society*, 136, 97–111.
- Sobral, G., Sookias, R. B., Bhullar, B. A. S., Smith, R., Butler, R. J., & Müller, J. (2016). New information on the braincase and inner ear of *Euparkeria capensis* Broom: Implications for diapsid and archosaur evolution. *Royal Society Open Science*, 3, 160072.
- Stocker, M. R., Nesbitt, S. J., Criswell, K. E., Parker, W. G., Witmer, L. M., Rowe, T. B., Ridgely, R., & Brown, M. A. (2016). A dome-headed stem archosaur exemplifies convergence among dinosaurs and their distant relatives. *Current Biology*, 26, 2674–2680.
- Sues, H.-D., Averianov, A. O., Ridgely, R. C., & Witmer, L. M. (2015). Titanosauria (Dinosauria, Sauropoda) from the Upper Cretaceous Bissekty Formation of Uzbekistan. *Journal of Vertebrate Paleontology*, 35, e889145-1–e889145-14.
- Sulej, T. (2010). The skull of an early Late Triassic aetosaur and the evolution of the stagonolepidid archosaurian reptiles. *Zoological Journal of the Linnean Society*, 158, 860–881.
- Székely, G., & Matesz, C. (1988). Topography and organization of cranial nerve nuclei in the sand lizard, *Lacerta agilis*. *The Journal of Comparative Neurology*, 267, 525–544.
- Taborda, J. R. A., Desojo, J. B., & Dvorkin, E. N. (2021). Biomechanical skull study of the aetosaur *Neoaetosauroides engaeus* using Finite Element Analysis. *Ameghiniana*, 58(5), 401–415. <https://doi.org/10.5710/AMGH.23.07.2021.3412>
- Trotteyn, M. J., & Haro, J. A. (2012). The braincase of *Chanaresuchus ischigualastensis* (Archosauriformes) from the Late Triassic of Argentina. *Journal of Vertebrate Paleontology*, 32, 867–882.
- Trotteyn, M. J., & Paulina-Carabajal, A. (2016). Braincase and neuroanatomy of *Pseudochampsia ischigualastensis* and *Tropidosuchus romeri* (Archosauriformes, Proterochampsia). *Ameghiniana*, 53, 527–542.
- von Baczko, M. B., & Desojo, J. B. (2016). Cranial anatomy and paleoneurology of the archosaur *Riojasuchus tenuisiceps* from the Los Colorados Formation, La Rioja, Argentina. *PLoS One*, 11, e0148575.
- von Baczko, M. B., Taborda, J. R., & Desojo, J. B. (2018). Paleoneuroanatomy of the aetosaur *Neoaetosauroides engaeus* (Archosauria: Pseudosuchia) and its paleobiological implications among archosauriforms. *PeerJ*, 6, e5456.
- von Wettstein, O. (1937-1954). Crocodylia. In W. Kiikenthal, T. Krurnbach, J.-G. Helmcke, & H. von Lengerken (Eds.), *Handbuch der Zoologie: Eine Naturgeschichte der Stämme der Tierreiches. Sauropsida: Allgemeines Reptilia, Aves* (Vol. 7, pp. 236–424). de Gruyter.
- Walker, A. D. (1961). Triassic reptiles from the Elgin area: Stagonolepis, Dasygnathus and their allies. *Philosophical Transactions of the Royal Society of London. Series B*, 244(709), 103–204.
- Werneburg, I., & Yaryhin, O. (2018). Character definition and tempus optimum in comparative chondrocranial research. *Acta Zoologica*, 100, 376–388.
- Witmer, L. M., & Ridgely, R. C. (2009). New insights into the brain, braincase, and ear region of tyrannosaurs, with implications for sensory organization and behavior. *The Anatomical Record*, 292, 1266–1296.
- Witmer, L. M., Ridgely, R. C., Dufeu, D. L., & Semones, M. C. (2008). Using CT to peer into the past: 3D visualization of the brain and ear regions of birds, crocodiles, and nonavian dinosaurs. In *Anatomical imaging* (pp. 67–87). Springer.

How to cite this article: von Baczko, M. B., Desojo, J. B., Gower, D. J., Ridgely, R., Bona, P., & Witmer, L. M. (2021). New digital braincase endocasts of two species of *Desmatosuchus* and neurocranial diversity within Aetosauria (Archosauria: Pseudosuchia). *The Anatomical Record*, 1–20. <https://doi.org/10.1002/ar.24798>